Sustainable Cities and Society 98 (2023) 104844

Contents lists available at ScienceDirect

Sustainable Cities and Society

journal homepage: www.elsevier.com/locate/scs

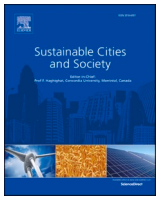

Water distribution system design integrating behind-the-meter solar under long-term uncertainty

Jiayu Yao [a,*], Wenyan Wu [a], Angus R. Simpson [b], Behzad Rismanchi [a]

[a] Department of Infrastructure Engineering, Faculty of Engineering and Information Technology, The University of Melbourne, Victoria, 3010, Australia
[b] School of Architecture and Civil Engineering, Faculty of Sciences, Engineering and Technology, The University of Adelaide, South Australia, 5005, Australia

ARTICLE INFO

Keywords:
Water distribution system
Behind-the-meter solar
Water demand uncertainty
Technology development uncertainty

ABSTRACT

Water distribution systems (WDSs) are important urban water infrastructure supporting a wide range of human activities. Due to the significant amount of energy consumed by the WDS throughout its lifespan, the operation of WDSs may have a significant impact on the environment, affecting the sustainable development of cities into the future. Behind-the-metre (BTM) solar photovoltaic (PV) system integration has been considered an effective way to reduce the impact of WDSs on the environment. However, solar PV technology is developing rapidly. Combined with long-term changes in water demand driven by population growth and urbanisation, the design of a WDS considering BTM solar has become a more challenging task. In this study, the co-design of WDS integrating BTM solar PV systems under changing future conditions in terms of water demand and solar PV technology development is investigated. It has been found that the BTM solar PV system and the potential development in solar PV technology effectively improve the robustness of WDS design under uncertain future water demand. The outcomes of this study can be extended to guide infrastructure design to provide sustainable infrastructure for future cities, and therefore cities can continue to support human activities in deeply uncertain future.

1. Introduction

Water distribution systems are essential components of urban water infrastructure, which plays a vital role in the sustainable development of cities. WDSs supply water with appropriate pressure from water sources to consumers to meet different needs in urban areas (National Research Council, 2007). This infrastructure is necessary for multiple human activities, such as maintaining health and well-being, and supporting industrial production and agricultural activities (EPA, 2022). However, the construction and operation of WDSs are recognised as the major driving forces for environmental change to the natural environment (Doyle & Havlick, 2009). Therefore, it is crucial to account for WDSs' potential impact on the natural environment and in turn on the sustainable development of cities and their ability to support future human activities when designing WDSs.

Pressurised distribution systems for water supply in urban areas usually consume significant amounts of energy, contributing to a large amount of greenhouse gas (GHG) emissions (Sharif et al., 2019). As reported by Coelho and Andrade-Campos (2014), around 7% of the total energy generation is consumed by distributing water every year globally. The energy consumption for distributing water can also contribute to non-negligible GHG emissions. For instance, emissions by water utilities account for approximately 1% of the total GHG emissions in the U.S. (Zib III et al., 2021). Due to the growing concern about the global energy crisis, and the intention to reduce GHG emissions and the related impact of climate change (Garcia et al., 2021), researchers have been working on reducing the energy usage and its related emissions for WDSs.

As a result, the 'energy-for-water' perspective has become a major research focus recently, when designing and operating the WDSs (Hamiche et al., 2016). These studies can be classified into three categories based on the energy supplied for WDSs: (1) studies aiming at reducing energy consumption and GHG emissions when designing the WDS (Luna et al., 2019; Wu et al., 2010); (2) studies considering energy saving from pump operations (Behandish & Wu, 2014; Marchi et al., 2012), energy recovery through micro hydro-turbines, pump as a turbine, etc. (Ávila et al., 2022; De Marchis et al., 2014; Sitzenfrei & Rauch, 2015; Tricarico et al., 2018), and energy efficiency improvement measures (Ramos et al., 2011); and (3) studies seeking renewable energy as sources of energy supply for the system, such as solar photovoltaic (Carrillo-Cobo et al., 2014; Giudici et al., 2019; Olcan, 2015) and wind (Rehman & Sahin, 2012). Instead of making adjustments on components

* Corresponding author.
E-mail address: jiayuy4@student.unimelb.edu.au (J. Yao).

https://doi.org/10.1016/j.scs.2023.104844
Received 21 April 2023; Received in revised form 23 June 2023; Accepted 1 August 2023
Available online 2 August 2023

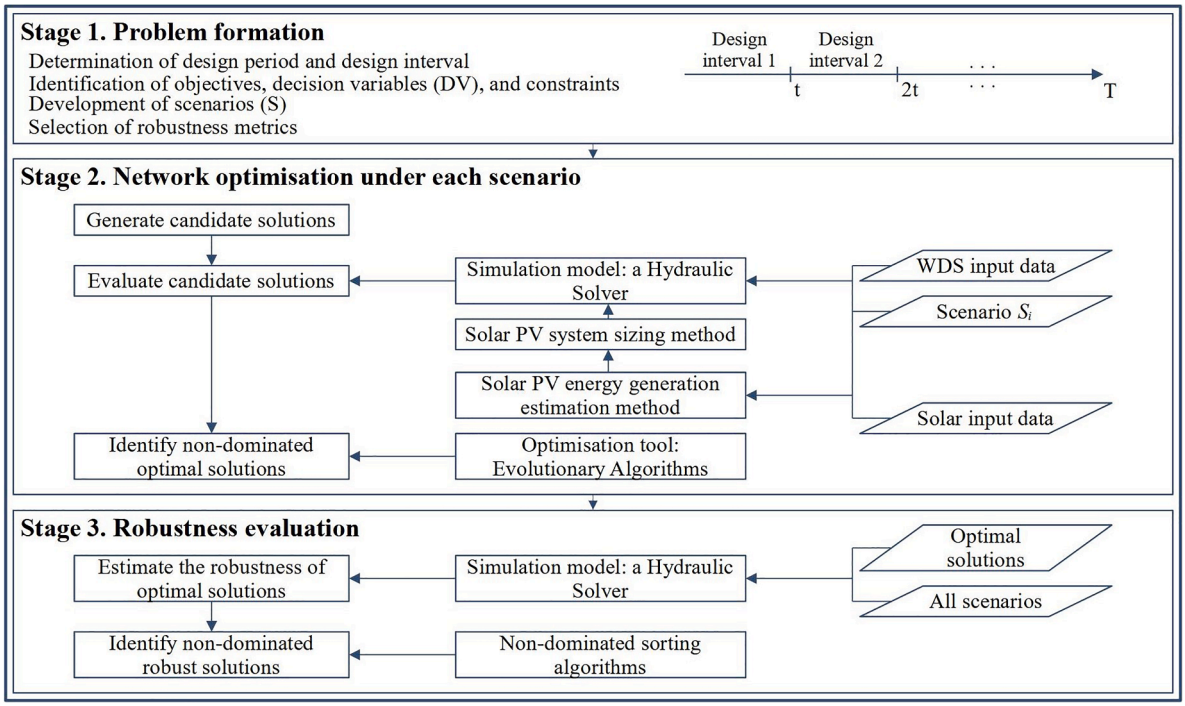

Fig. 1. Overview of the methodology.

within the WDS, renewable energy integration focuses on improving the system energy performance from an energy supply side of view. According to Garcia et al. (2021), renewable energy integration into WDSs could effectively reduce the systems' dependence on traditional energy sources and thus correspondingly reduce the related GHG emissions. Moreover, with renewable integration, the impact of an uncertain energy market in the future will be minimised. This leads to the installation of behind-the-metre (BTM) solar systems as an alternative or additional energy supply source for WDSs (Zhao et al., 2023). Such onsite energy generation systems have been considered as an effective way to lower the environmental impact as well as manage the economic cost of WDSs (Bayram & Ustun, 2017; Garcia et al., 2021). In addition, with locally energy generated by BTM solar consumed onsite and excess electricity generated provided to the central grid, the resilience and security of the energy grid could be improved (Angizeh et al., 2021).

When integrating BTM solar photovoltaic (PV) systems into WDSs, one major consideration is the relationship between the energy supplied by the BTM solar and the energy consumed by the WDS. Since solar resources are highly intermittent, this leads to a large variation in energy supplied by solar generation (Gowrisankaran et al., 2016). Meanwhile, the pumping energy required by the WDS exhibits variation as well, as the energy requirement of the system depends largely on the amount of water to be delivered, which could vary significantly even within a day (Letting et al., 2017). Therefore, it is important to view these two systems together as a combined system, to include the interactions of energy demand-supply balance inside the design process. There has been limited research on the co-design of WDS and BTM solar systems, with a focus mostly on the design of WDSs (Zhao et al., 2023).

The co-design of a WDS integrating BTM solar energy system needs to consider not only future changes in water demand, but also the potential impact of solar PV technology development. WDSs have relatively long service lifespans (National Research Council, 2005), and the water demand may change significantly under the impact of long-term drivers of population growth and urbanisation (Okello et al., 2015; Wu et al., 2020; WWAP, 2019). Therefore, instead of designing and optimising WDSs under certain pre-determined future conditions (Simpson et al., 1994; Walters et al., 1999), recent studies have started to take into account the deeply uncertain water demand changes in the design of WDSs in the distant future. There has been considerable research investigating the impact of future changes in water demand on the planning, design and operation of WDSs (Basupi & Kapelan, 2015; Creaco et al., 2015; Cunha et al., 2019, 2020; Marques et al., 2015a, 2015b, 2017, 2018; Tsegaye et al., 2020; Zhang et al., 2013).

However, there has been very limited research considering long-term uncertainty associated with solar PV technologies. Solar PV modules have gone through significant changes over the past several decades. The solar cell efficiency has more than doubled in the past 20 years (National Renewable Energy Laboratory, 2022; Shubbak, 2019), and the solar panel unit cost has been driven down to less than 1/15 compared to 1980′s conditions (Gul et al., 2016; Victoria et al., 2021). Due to the relatively short service lifespan of solar PV panels of 20–25 years, the cost and efficiency of replaced solar panels in the future are highly uncertain. The long-term uncertainty related to solar PV technology may then lead to variations in the generation performance of the BTM solar system. Consequently, solar PV technology development uncertainty and its impact on the co-design of the WDS with the BTM solar system should also be taken into account for the co-design of WDSs integrating BTM solar.

To inform the design of WDSs for future cities and design these systems to be robust as well as resilient to future changes, this study is proposed to explore the impact of long-term water demand changes and solar PV technology development on the co-design of BTM solar-integrated WDSs. Two benchmark case studies have been applied to investigate: (1) the impact of different sources of long-term uncertainty on the design of BTM integrated WDSs, and (2) the impact of different robustness metrics on the identified robust solutions. The rest of this paper is structured as follows, Section 2 introduces the general methodology of this work, which includes the method developed for the co-design of the BTM solar-integrated WDS and the method used to account for long-term uncertainty considered in this study. The detailed case study descriptions, including the formation of the multi-objective optimisation problem and the simulation and optimisation methods used, are presented in Section 3. Section 4 includes the results and discussion, and Section 5 concludes the paper.

2. Methodology

2.1. Overview of the co-design of WDS integrating BTM solar system

The primary focus of this study is to investigate the impact of different sources of long-term uncertainty (i.e., water demand changes and changes in solar PV technology into the future) on the co-design of BTM solar PV integrated WDSs. The general design approach that has been applied is shown in Fig. 1.

The first stage of this approach is problem formation, which is generally made up of three parts. First, the WDS optimisation problem is formulated. This involves determining the design period T, design interval t (e.g., a design period of 60 years is divided into 3 design intervals of 20 years), and the simulation timestep ΔL, identifying the WDS's characteristics such as nodal water demands, pipe lengths, etc. These provide the required information for the hydraulic simulations and related calculations of the WDS. Moreover, the decision variables $DV = \{DV_1, DV_2, \ldots DV_n\}$ (e.g., pipe sizes) within the WDS that need to be decided upon the optimisation and constraints to be considered during the optimisation are identified. The optimisation objectives represented by performance metrics in terms of the system's economic, environmental performances are to be determined as well. Second, in addition to the design and optimisation of WDS, method for determining the BTM solar PV system generation capacity is developed. In this study, the solar PV generation capacity is considered as a dependant variable of WDS's design and energy requirements, and it is determined with consideration of the cost and benefits of the integrated BTM solar system (Section 2.2.1). Then the actual energy generated from each solar PV system can be determined based on solar resources availability at the installation location (Section 2.2.2). Lastly, scenarios, i.e., $S = \{S_1, S_2, \ldots S_n\}$, are developed to account for long-term uncertainty related to the BTM integrated WDS. Each scenario may lead to one distinct plausible future condition, and all the scenarios are viewed as equally likely to occur into the future (Kwakkel et al., 2010). The different scenarios developed with combinations of different changes to long-term drivers represent the possible range of the future conditions for the integrated system under multiple sources of long-term uncertainties (Lempert, 2003; Maier et al., 2016). There are different sources of long-term uncertainty that may affect the BTM solar PV integrated WDS in the distant future. Long-term uncertainty associated with water demand and solar PV technology development are identified as two major sources of uncertainty that may impact the co-designed system. The scenarios developed based on long-term changes of water demand, and changes in solar PV unit cost and conversion efficiency (referred to as 'solar PV technology development') are discussed in Sections 2.3.1 and 2.3.2, respectively.

In the second stage, the BTM solar integrated WDS is optimised under each developed scenario S_i using evolutionary algorithms (Maier et al., 2019). During the optimisation process, candidate solutions that are combinations of decision variables values are generated. For each generated candidate solution, the hydraulic simulation of the WDS is conducted using a hydraulic solver. In addition, the hydraulic simulation provides relevant information for determining the integrated BTM solar system capacity, and thus the defined optimisation objectives are able to be calculated. The trade-off between optimisation objectives in terms of a Pareto front will then give a set of non-dominated solutions, which are identified as optimal design solutions for the future scenario considered. This optimisation process is repeated for all the scenarios developed in the first step, and thus yields one set of optimal design solutions for each scenario.

To select design solutions that could perform well under a range of plausible future scenarios, in the third stage, the performances of these optimal design solutions are evaluated using various robustness metrics (McPhail et al., 2018). In this stage, all the optimal solutions obtained are first simulated under all future scenarios developed using the hydraulic solver. The optimisation objectives in terms of performance metrics for each scenario are then be calculated using the simulation data, and the values of different robustness metrics that are calculated based on the solutions' performances across all scenarios are obtained. Finally, the Pareto-optimality of previously obtained optimal solutions (i.e., optimal solutions under all different scenarios) in terms of the values of each robustness metric considered can be assessed, leading to a single set of non-dominated solutions for each robustness metric under all scenarios representing long-term uncertainty. The detailed implementation of this methodology over the case study networks are discussed in Section 3.

In this study, a design period of 60 years is assumed, starting from 2020 until 2079. Considering the lifespan of pumps and solar PV panels in the integrated system, the design period is further divided into three 20-year design intervals. The pumps and solar PV systems are to be resized at the start of each design interval. In addition, location-specific information required in the optimisation and simulation process are hypothetical and simplified. For illustration of the methodology, data such as solar resources availability and water demand patterns based on Melbourne, Australia's conditions have been adopted.

2.2. Integration of BTM solar PV systems

In this study, a solar PV system is integrated into the WDS as an additional source of energy supply. To maximise the benefits of the integrated BTM solar system, use of the electricity generated from this system is prioritised over energy from the centralised electricity grid. When the solar energy generated cannot satisfy the energy demand of pumping in the WDS, additional energy is sourced from the centralised electricity grid. Meanwhile, the excess solar energy generated will be sold back to the centralised grid if the solar generation is not fully utilised by the WDS. This is a common arrangement between energy providers and water utilities with BTM solar in Australia (Zhao et al., 2023). The BTM solar PV system generation capacity is considered as a dependant variable, which is determined by the WDS's configuration and pumping energy requirement. This is to make sure the best BTM solar PV system option is used for each potential WDS solution under evaluation in the optimisation process. The feed-in-tariff has been taken as zero in this study for determining the size of the BTM solar PV system to avoid oversizing of the system for maximising the economic benefits by selling excess energy generated from BTM solar systems back to the centralised grid. Moreover, by assuming a zero feed-in-tariff, the outcomes from this study are more widely applicable for the design and optimisation of WDSs regardless of if there is an agreement between water utilities and energy providers to sell excess energy back into the grid. Therefore, for each WDS candidate solution, a BTM solar PV system is sized based on the characteristics of the specific network to optimally meet the energy demand by the network.

2.2.1. Solar PV system sizing method

The determination of solar PV generation capacity has been formulated as a single-objective optimisation where the economic cost directly related to the BTM solar PV system is minimised. To eliminate the impact of the cost of pipes and pumps, which are far beyond the cost associated with pumping energy, only the economic cost related to energy for pump operation of the system will be minimised. Thus, the Total Energy-related Cost (TEC) is defined and formulated as:

$$TEC = \begin{cases} SC + PV(OC), & for\ stage = 1 \\ PV(SRC) + PV(OC), & for\ stage > 1 \end{cases} \quad (1)$$

where SC represents the capital cost for the solar PV system; $PV(OC)$ is the present value of operational cost of the water distribution network, which accounts for the cost of energy taken from the grid that cannot be fully supplied by the solar PV system; SRC refers to solar panel replacement cost.

An inequality constraint is applied to the optimisation to ensure the solar PV system is cost-effective, and the constraint is given as a Benefit-

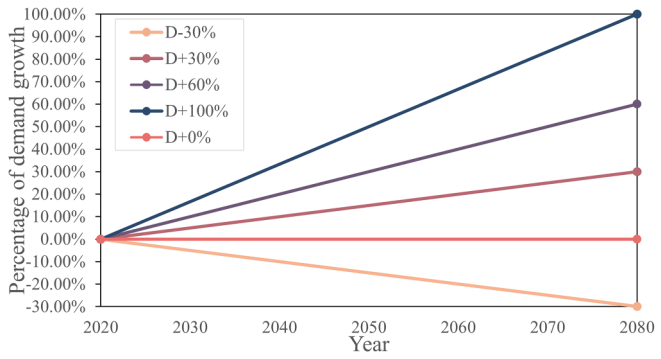

Fig. 2. Water demand change trajectories.

Cost-Ratio (*BCR*):

$$BCR = \begin{cases} \dfrac{PV(OCS)}{SC} - 1 \geq 0, \ for\ stage = 1 \\ \dfrac{PV(OCS)}{PV(SRC)} - 1 \geq 0, \ for\ stage > 1 \end{cases} \quad (2)$$

where *OCS* represent the operational cost savings due to the solar PV integration, which is calculated as the equivalent cost of the energy supplied by the solar PV system energy generation.

The BTM solar PV system size is determined for each design interval separately. The operational cost represents the sum of the present discounted cost spent on electricity bought from the grid within each design interval of 20 years. The capital cost of the solar PV system is considered as one-off payment that only occurs at the beginning of each design period.

The non-linear programming method of Sequential Least Squares Programming (SLSQP) was chosen to solve the single-objective optimisation problem (Kraft, 1988). In this study, a python PyPi package called 'Scipy', which offers the application of the SLSQP method, was adopted for the optimisation of solar PV system capacity (Virtanen et al., 2020).

2.2.2. Solar PV system energy generation estimation method

In this study, solar PV system generation is estimated hourly throughout the design period as a general representation of intermittent solar resources. First, the total annual solar PV system energy generation is calculated based on the approximate solar PV unit generation for the location of installation and the solar PV generation capacity to be installed. Second, the total amount of generation is disaggregated into each month of the year based on the interannual solar resources variation. It is assumed that there is no variation in generation within a month, so the total monthly generation is equally disaggregated to each day in a month. And lastly, 24 h solar PV generation patterns for different calendar months are developed by further disaggregating daily generation to each hour of the day. The hourly solar PV system generation is formulated as:

$$SG_{m,\,t} = (SpC \times uSG \times\ 365)\ \times SGMonMulti_m \times SGDiuMulti_t \quad (3)$$

where *SpC* is the solar PV system generation capacity, and *uSG* represents the unit generation for solar panels at the installation location (kWh/day); *SGMonMulti* is the disaggregation multiplier for month *m*, while *SGDiuMulti* stands for disaggregation multiplier for hour *t* within a day.

Global Horizontal Irradiation (GHI) is the most important and widely used variable for estimating the amount of solar received by solar panels in solar PV potential models (Bolinger et al., 2016; Energy Sector Management Assistance Program, 2020). Therefore, in this study, historical GHI data is used to characterise the general seasonal variation in solar PV system generation. It is assumed that solar PV system generation is proportional to GHI measured at the location. The monthly and hourly disaggregation multipliers are then be developed based on historical GHI data.

As discussed in Section 2.1, GHI and solar PV generation data of Melbourne, Australia is used in this study to develop the solar PV generation patterns for the case studies. The average daily production of a solar PV system located in Melbourne with a capacity of 1 kW is around 3.6 kWh (Clean Energy Council, 2020). The ageing of the solar PV system is neglected so that during the operation lifespan the generation efficiency of solar panels is assumed as constant. Disaggregation calculations are averaged across a 5-year (2016–2020) time series of hourly GHI data (Data source: NSRDB (National Solar Radiation Database, 2022)) to eliminate the impact of extreme years. The developed monthly and diurnal solar PV generation patterns are illustrated in Fig. A.1 and Fig. A.2.

2.3. Scenario development

2.3.1. Changes in future water demand

Water demand uncertainty is the first source of long-term uncertainty considered in this study. Two major driving forces that may lead to the increase in urban water demand include population growth (Boretti & Rosa, 2019; Okello et al., 2015; WWAP, 2019) and climate change (Gato et al., 2007; State of Victoria, 2016). Meanwhile, wastewater recycling techniques and decentralised water supply such as rainwater tanks may provide additional water sources for urban water supply and may thus reduce the burden on traditional centralised water distribution systems (Arora et al., 2015). Five future water demand change trajectories with different rates of change (from −30% to +100%) have been developed to cover potential long-term changes in demand mentioned above.

As illustrated in Fig. 2, the water demand trajectories include: (1) the baseline trajectory (i.e., *D*+0%) where the demand is not changing across the design period; (2) the demand decrease trajectory (i.e., D-30%) that assumes alternative sources of water supply could effectively reduce the urban area's reliance on the centralised WDS, and the water demand will be 30% less than the demand at the design starting point; (3) three growth trajectories (i.e., *D*+30%, *D*+60%, and *D*+100%) with water demand increased to 130%, 160% and 200% compared to the demand in 2020 (i.e., the design starting point).

2.3.2. Changes in solar PV technology

Another major source of long-term uncertainty considered in this study is the uncertainty associated with the future development of solar PV units. This mainly results in the uncertainty in future cost (Green, 2001; International Renewable Energy Agency, 2019) and conversion efficiency (Green, 2001; International Renewable Energy Agency, 2019; National Renewable Energy Laboratory, 2022) of solar PV panels that may affect the co-design of the BTM solar integrated WDSs. Three solar PV technological development trajectories are developed to represent: (1) the no technological change case (i.e., $T_{Const.}$, to be used as a baseline trajectory for comparison), where the unit cost and conversion efficiency of solar PV panels remain constant into the future; (2) the development of conventional crystalline silicon cells (i.e., $T_{Conv.}$) that represents a steady improvement in cost and conversion efficiency of the widely applied crystalline silicon solar cells; and (3) the development of advanced 3rd generation solar cells (i.e., $T_{Adv.}$). The three solar PV technology development trajectories developed are shown in Fig. 3. It is assumed that once the solar PV system is installed, the cost and conversion efficiency will not change during its service lifespan of 20 years.

2.3.3. Summary of scenarios

In this study, 15 scenarios have been developed based on the different combinations of the five demand change trajectories and three solar PV technology development trajectories into the future. These 15 scenarios are summarised in Fig. 4. Each cell in the figure shows one scenario, which represents a specific combination of one demand change

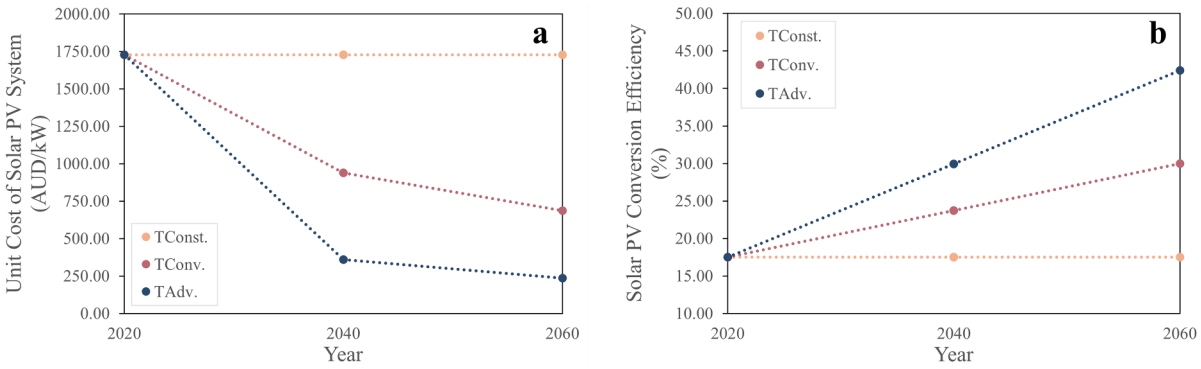

Fig. 3. Solar PV technology development trajectories (a) solar PV unit cost trajectories and (b) solar PV conversion efficiency trajectories.

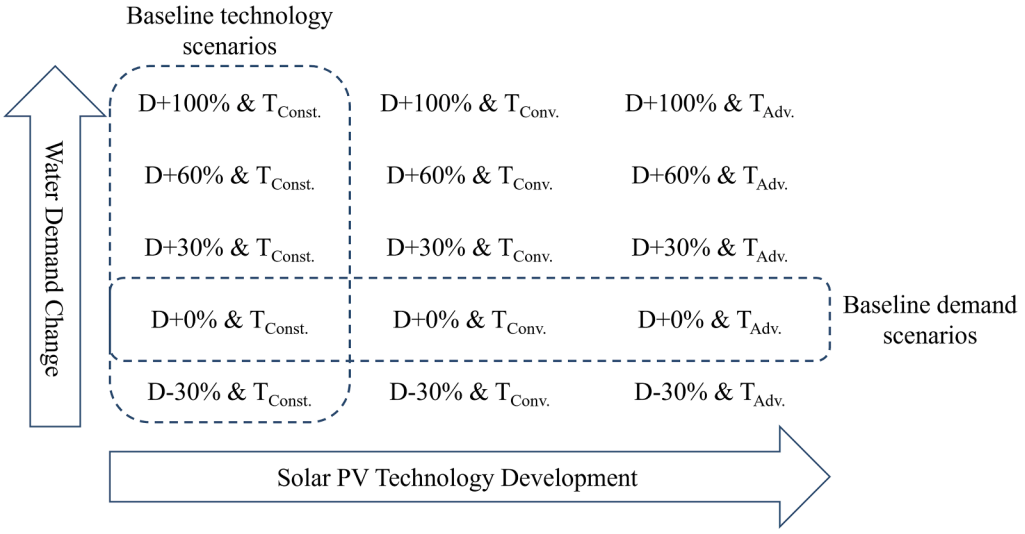

Fig. 4. Summary of the 15 scenarios.

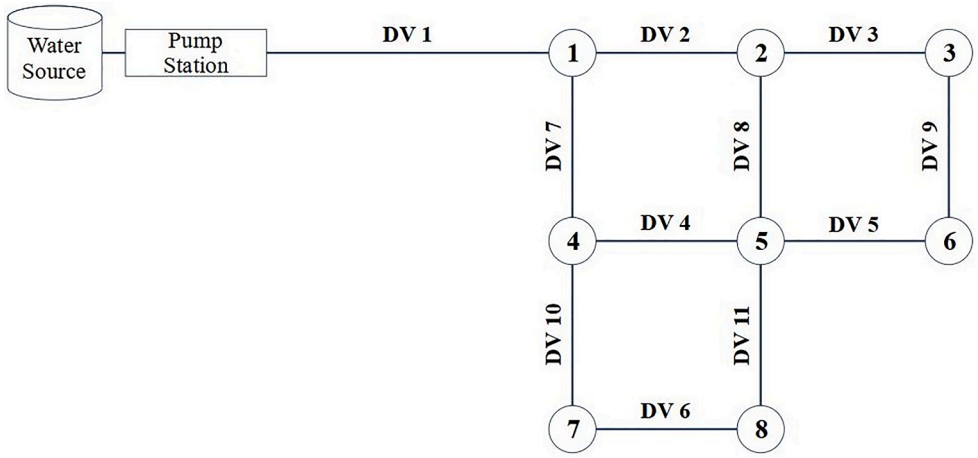

Fig. 5. Modified Net1 network (Pipe length: DV1=3209 m; DV2-DV11=1609 m; Nodal base demand: Node 3,7,8 = 7 L/s; Node 1,2,4,6 = 10 L/s; Node 5 = 13 L/s).

trajectory and one solar PV technology development trajectory. For instance, the cell at the top right corner (i.e., D-30% & $T_{Adv.}$) shows the future conditions that water demand is reduced by 30% by the end of the design period, while advanced solar PV units are available for the solar PV system within the design period. Amongst the 15 scenarios, two groups of scenarios named as baseline technology scenarios (i.e., D-30% & $T_{Const.}$, D+0% & $T_{Const.}$, D+30% & $T_{Const.}$, D+60% & $T_{Const.}$, D+100% & $T_{Const.}$) and baseline demand scenarios (i.e., D+0% & $T_{Const.}$, D+0% & $T_{Conv.}$, D+0% & $T_{Adv.}$) that represent baseline trajectories of the two sources of uncertainty correspondingly, are considered in the robustness evaluation stage. Baseline technology scenarios include five scenarios where solar PV units' cost and conversion efficiency remain unchanged, while all five demand change trajectories considered. Thus, investigation of results from this group of scenarios explains the impact of

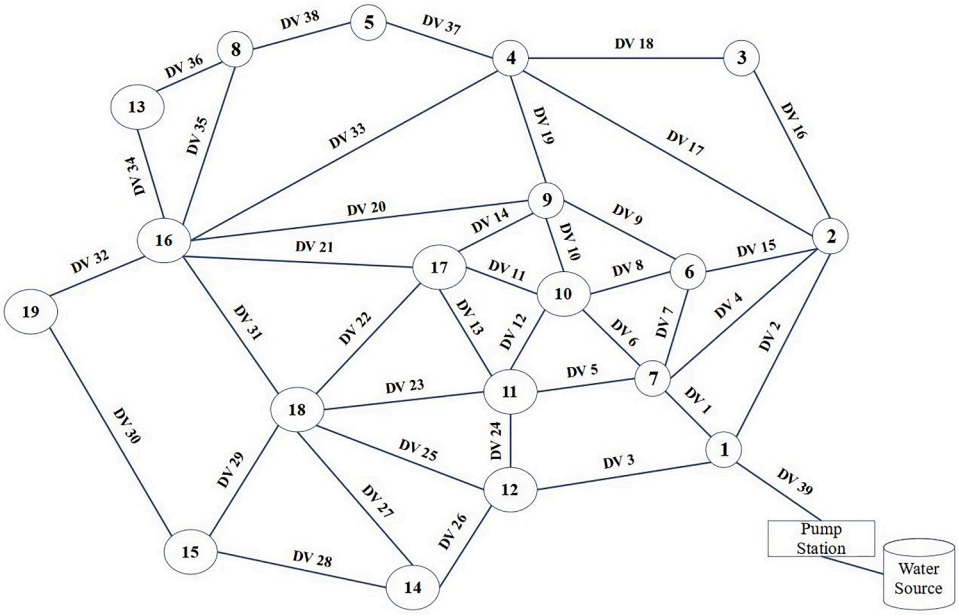

Fig. 6. Modified Anytown network (Pipe length: DV1-DV3, DV32-DV33=3658 m; DV4=2743 m; DV34-DV38=1829 m; DV5-DV31=183 m; DV39=10 m; Nodal base demand: Node 2,3 = 13 L/s; Node 14–17,19=25 L/s; Node 6,7,9,11,12=32 L/s; Node 4,5,8,13=38 L/s; Node 10,18=63 L/s).

demand uncertainty on the co-design of BTM integrated WDSs. Similarly, three baseline demand scenarios' results provide insight into the impact of solar PV technology development uncertainty on the design.

3. Case study

3.1. Case study networks

Two hypothetical case studies are considered in this study. First, the case study network 1 is modified from the example network Net 1 provided by EPANET (Open Water Analytics, 2022a), as shown in Fig. 5. The modified Net 1 network, which consists of 11 pipes and 8 demand nodes, is supplied by a pump station located near the source of water. The base demand at demand nodes varies from 7 L/s to 13 L/s, with a total base demand equal to 74 L/s, and water is pumped directly from the source to each individual demand node to ensure the demands are always met during the design period.

The case study network 2 is modified from the Anytown network, which is a hypothetical network proposed by Walski et al. (1987). The layout of the network is shown in Fig. 6. The network is composed of 19 demand nodes connected by 39 pipes, and the nodal base demand changes from 13 L/s to 63 L/s. The pump station is operated 24 hours per day to deliver water from the source to each demand node.

3.2. Multi-objective optimisation objective function formulation

The water distribution network design considering behind-the-metre solar energy integration under long-term uncertainty is formulated as a multi-objective optimisation problem. The sizes of pipes are taken as the decision variables of the optimisation problem. In this problem, a minimum allowable pressure head of 28 meters of water is set to be satisfied at all times (Ghorbanian et al., 2015). The variable speed pump handles the pressure head constraint, as discussed in Appendix B.

3.2.1. Minimisation of total life cycle cost (TLCC)

The Total Life Cycle Cost (TLCC) of the system is formulated as:

$$TLCC = CC + PV(PRC) + PV(SRC) + PV(OC) \tag{4}$$

where CC is the capital cost, PRC and SRC are the pump station refurbishment and solar panel replacement costs at the later design intervals, respectively, and OC represents the operational cost induced by pump operation during the design period.

3.2.1.1. Capital cost (CC). The Capital Cost (CC) is given by the following equation:

$$CC = \sum_{i=1}^{No.\ of\ Pipes} D_i L_i + PC + SC \tag{5}$$

where the capital cost for pipes is calculated using the unit cost of pipe i (D_i, in \$/m) and the length of the pipe (L_i, in meters); PC is the cost for the pump station and initial pump set to be installed at the beginning of the design, and SC is the capital cost for the solar panel system. The unit cost for DICL pipes with different commercial sizes is adopted from the Department of Primary Industries (2014). The pump station and initial pump set capital cost are calculated based on the maximum pump power required by the network (Department of Primary Industries, 2014). The estimated costs for commercial solar PV systems are provided by Clean Energy Council (2020) for various solar PV capacity sizes, the capital costs for different solar PV system sizes used in this study are linearly interpolated or extrapolated based on the reference data.

3.2.1.2. Pump station refurbishment cost (PRC) and solar panel replacement cost (SRC). The service lifespan of pumps and solar PV units is assumed to be 20 years (Clean Energy Council, 2020; Water Services Association of Australia, 2011). Therefore, the pumps and solar PV units are replaced every 20 years during the whole design period of 60 years, and the replacements happen at the beginning of each design interval. The Pump station Refurbishment Cost (PRC) and Solar panel Replacement Cost (SRC) are calculated as:

$$PV(PRC) = \sum_{t_R}^{T} PuC_{t_R} \times \frac{1}{(1+i)^{t_R}} \tag{6}$$

$$PV(SRC) = \sum_{t_R}^{T} SpC_{t_R} \times \frac{1}{(1+i)^{t_R}} \tag{7}$$

where PuC and SpC are the cost for the new pumps and new solar panels

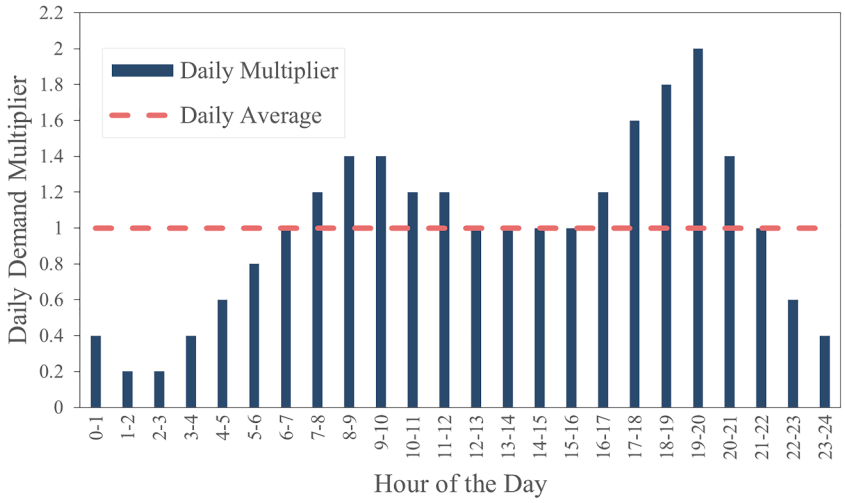

Fig. 7. Diurnal water demand pattern.

Table 1
Seasonal water demand variations.

Months of the Year	Monthly Demand Multiplier
January, February, and March	1.23
April, May, and June	1.03
July, August, and September	0.82
October, November, and December	0.92

to be installed at year t_R, i is the discount rate, which converts the future payments to present values. The sum of pump replacement and pump station refurbishment costs is assumed to be 70% of the capital cost for the pump station and pump set with the same pump power (Department of Primary Industries, 2014). Although the unit costs for solar PV units are expected to keep decreasing driven by technological development, as the unit price has decreased by up to 90% in the past decade (Wang et al., 2021), the replacement and refurbishment cost is calculated and discounted based on current conditions (at the starting point of the design period). In this study, a 6% discount rate is assumed for the present value calculations based on the Australian condition (Abelson & Dalton, 2018; Terrill & Batrouney, 2018).

3.2.1.3. Operational cost (OC). The Operational Cost (OC) over the design period is given below:

$$PV(OC) = ET \times \sum_{t=1}^{No.\ of\ Years} TGEC_t \times \frac{1}{(1+i)^t} \tag{8}$$

where, ET represents the electricity tariff for energy purchased from the grid, which is assumed as \$0.23/kWh for the whole design period, and it is calculated based on the Victoria default price with daily price fluctuation being neglected (Essential Services Commission, 2021); and $TGEC_t$ is the total grid energy consumed by the network during year t.

3.2.2. Minimisation of total grid energy consumed (TGEC)

The Total Grid Energy Consumed (TGEC) is formulated as:

$$TGEC = \sum_{y=1}^{No.\ of\ years} \sum_{m=1}^{12} \left(Days_m \times \sum_{h=1}^{24} GEC_{h,m,y} \right) \tag{9}$$

where $Days$ is the number of days in month m, and $GEC_{h,m,y}$ represents the hourly grid energy consumed for month m in year y.

The grid energy consumed (GEC) for a particular hour is calculated using the following equation:

$$GEC_t = \begin{cases} 0 & , \ when\ PuE \le SG \\ PuE_t - SG_t, & when\ PuE > SG \end{cases} \tag{10}$$

where, PuE_t is the pump energy consumed for time t, which is calculated by the pump head and flow delivered at that time, using $PuE = \gamma Q H_P / \eta$ (γ – specific weight of water, 9789 N/m^3 for water at 20 °C, Q – flow at time t in m^3/s, H_P – pump head at time t in m, and η – pump efficiency, in this case, a combined pump and motor efficiency of 0.8 is assumed); SG_t is the solar PV system generation at time t, which is estimated based on the solar PV system size and solar resources available at the particular time.

3.3. Water demand patterns

To characterise the networks' daily and seasonal water demand variation, a diurnal water demand curve has been developed for each season based on Melbourne's water consumption. In other words, there are in total 4 demand diurnal curves that have been developed for both case studies considered.

The water demand at each demand node in a water distribution network is assumed to follow the same diurnal and seasonal water demand variation pattern. The diurnal and seasonal variations of water demand are represented as hourly and monthly multipliers applied to the base demand of each demand node. The hourly water demand at a certain demand node has been calculated using:

$$WD_{n,\ m,\ t} = BD_n \times WDDiuMulti_t \times WDMonMulti_m \tag{11}$$

where, BD_n represents the base demand of node n; $WDDiuMulti_t$ is the aggregation multiplier for hour t, and $WDMonMulti_m$ is the aggregation multiplier for month m.

This study adopts a typical daily water demand pattern for Melbourne suburbs to characterise the demand variation within a day in this region (Gato-Trinidad & Gan, 2012; Roberts, 2005). It is assumed that there is no variation in the diurnal water demand pattern amongst different seasons, and that water demand patterns change in the long-term caused by improved water-efficient technology, behavioural changes of users or other factors are neglected (Beal & Stewart, 2014; Gato-Trinidad & Gan, 2012). Fig. 7 shows the water demand diurnal pattern with a 1-hour timestep, which has been applied in the network's Extended Period Simulation (EPS).

To account for seasonal water demand variation, monthly multipliers for the four seasons have been generated, as shown in Table 1. The monthly multipliers are developed based on previous research on

Table 2
Robustness metrics considered.

Robustness metric	Statistical characteristics	
	Average of performances	Range of performances
Mean-variance (Kwakkel et al., 2016)	✓	✓
Hurwicz optimism-pessimism rule (Hurwicz, 1951)	✓	
Undesirable deviations (Kwakkel et al., 2016)		✓

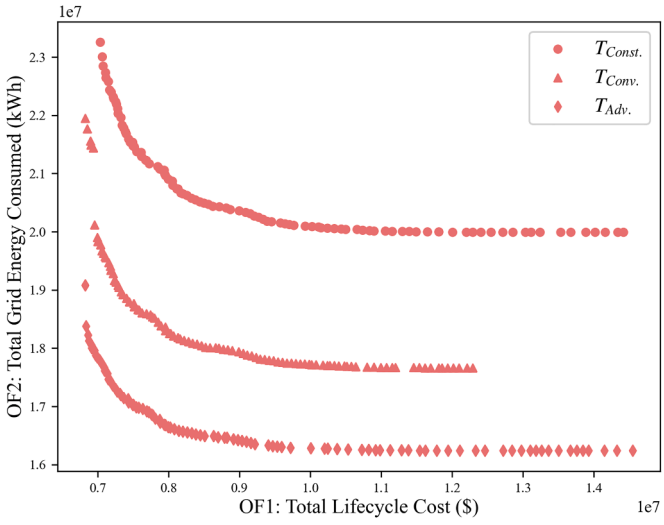

Fig. 8. Optimisation trade-offs under three baseline demand scenarios (Net1) (D+0% & $T_{const.}$, D+0% & $T_{conv.}$ and D+0% & $T_{Adv.}$).

household water use variability for Melbourne (Rathnayaka et al., 2014). The monthly multipliers are assumed to remain constant for the whole design period.

3.4. Optimisation and hydraulic simulation tools

The multi-objective optimisation problem has been conducted using the Non-dominated Sorting Genetic Algorithm (NSGAII), an optimisation algorithm that has been extensively applied in the planning and design of water distribution systems (Deb et al., 2002). In this study, a python PyPi package called 'pymoo', which offers different optimisation algorithms including the NSGAII, has been applied in designing the networks (Blank & Deb, 2020).

The extended-period simulations (EPS) of water distribution networks were conducted using the EPANET 2.2 Programmer's Toolkit (Rossman, 2000), and the python package called 'owa-epanet 2.2.4' which is a python wrapper for the EPANET toolkit library originally written in C (Open Water Analytics, 2022b). The simulation timestep for an EPS has been set as 1 hour, and the simulation length for one EPS is 24 hours, which was determined by the diurnal water demand pattern applied for the network. Considering the seasonal water demand variation, 12 EPSs with 24 hours length, have been conducted for one particular year within the design period. Moreover, since the water demand is changing annually under the water demand growth scenarios, the simulations have been repeated every year across the whole design period of 60 years. The detailed simulation method for variable speed pumps is discussed in Appendix B. The ageing impact of DICL pipes has been neglected in the simulation of the networks, and a pipe roughness of 100 (Hazen-Williams coefficient) has been assumed for all pipes within the network (PVC Pipe Association, 2017; Rossman, 2000).

3.5. Robustness evaluation

Robustness provides system performance evaluation under a range of plausible future conditions, and a robust solution is the solution that performs consistently well under these conditions (Maier et al., 2016). However, a number of robustness metrics have been developed that focus on assessing system performance in different ways, in terms of how performance metrics are used, how many scenarios are considered, and how the robustness calculation is conducted (McPhail et al., 2018). Therefore, three robustness metrics with totally different focuses have been selected in this study to include the impact of robustness metrics selection on the design results, as summarised in Table 2.

As shown in Table 2, the first robustness metric considered in this study is Mean-variance, which is calculated by multiplying the average performance of the solution across all the scenarios and the range of its performances. The Hurwicz optimism-pessimism rule calculates the weighted sum of the best and worst performances, providing characteristic similar to the solution's average performance. As there is no preference for either more optimistic results or more pessimistic results, in this research, the same weightings have been applied to the best and worst performances (i.e., 0.5 has been assigned for both performance values) for the calculation of Hurwicz optimism-pessimism robustness. In comparison, the Undesirable deviations assesses the range of the worst half of performances (i.e., the undesirable performances), and expresses the deviations in terms of the sum of their deviations from the median performance.

4. Results and discussion

4.1. Impact of different sources of long-term uncertainty on BTM integrated WDSs design

Optimisations of the BTM solar integrated case study WDSs have been conducted under (1) five baseline technology scenarios (i.e., D-30% & $T_{const.}$, D+0% & $T_{const.}$, D+30% & $T_{const.}$, D+60% & $T_{const.}$, and D+100% & $T_{const.}$), (2) three baseline demand scenarios (i.e., D+0% & $T_{const.}$, D+0% & $T_{conv.}$ and D+0% & $T_{Adv.}$), and (3) all 15 scenarios considering various changes in demand and solar PV technology development. Fig. 8 shows the optimisation trade-offs between the two objective functions of TLCC and TGEC for the Net1 network under the three baseline demand scenarios. The optimisation trade-offs under the other groups of scenarios for both case studies are illustrated in Fig. C.1 – Fig. C.5 in Appendix C.

As shown in Fig. 8, with the increasing improvements in solar technology into the future, the Pareto trade-off which is composed of the non-dominated design solutions generally moves downwards, indicating reduced energy consumption from the centralised electricity grid. This result is intuitive, as the development of solar PV technology will reduce WDS's energy consumption that are purchased from the grid.

To further investigate the impact of solar PV technology development on the detailed design of the WDS, heatmaps showing the selection of pipe sizes of the optimal solutions obtained under the three baseline demand scenarios (i.e., D+0% & $T_{const.}$, D+0% & $T_{conv.}$ and D+0% & $T_{Adv.}$) for Net1 network are presented in Fig. 9. The colours indicate the probability of selection of the pipes' sizes in the Net1 network for all the optimal solutions obtained under the three baseline demand scenarios. As demonstrated in Fig. 9, the selections of pipe sizes for optimal solutions optimised under the baseline demand scenarios are almost identical. Though, there are still some mismatch of pipe diameters selected amongst three different baseline demand scenarios. For instance, for results obtained under the scenario where development of advanced solar PV units is expected (i.e., D+0% & $T_{Adv.}$) and no technology development (i.e., D+0% & $T_{const.}$), the pipe linking node 1 and 5 (i.e., DV2) has a higher probability of being sized larger than 500 mm compared to those optimal solutions optimised under development of advanced solar PV units scenario (i.e., D+0% & $T_{conv.}$). Meanwhile, for

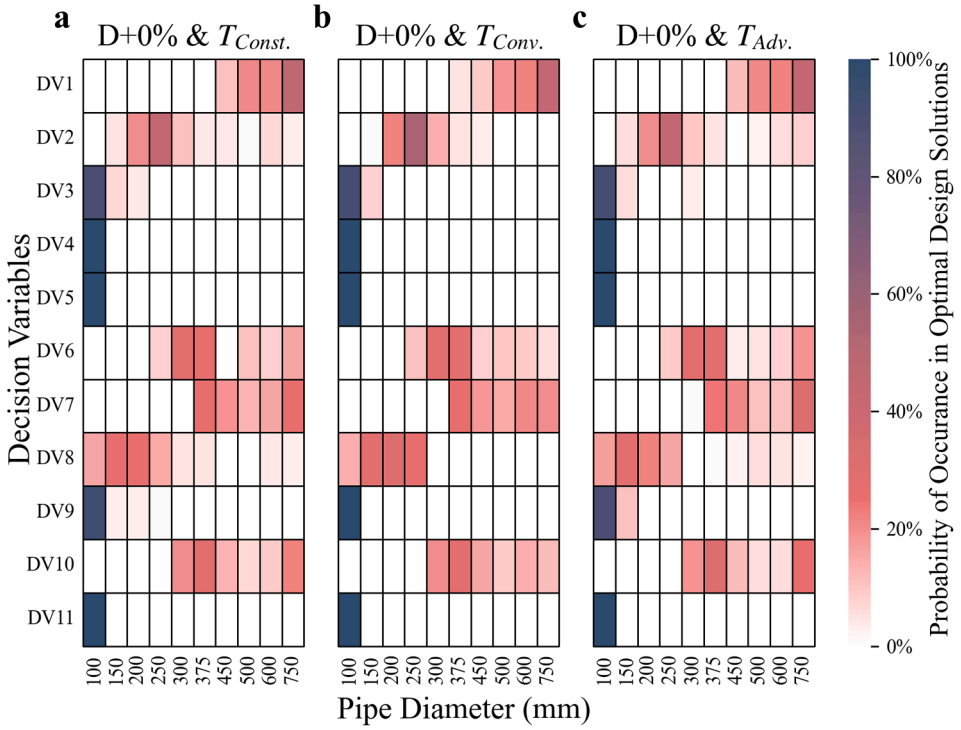

Fig. 9. Comparison of optimal solutions obtained under (a) D+0% & $T_{Const.}$ (b) D+0% & $T_{Conv.}$ (c) D+0% & $T_{Adv.}$ (Net1).

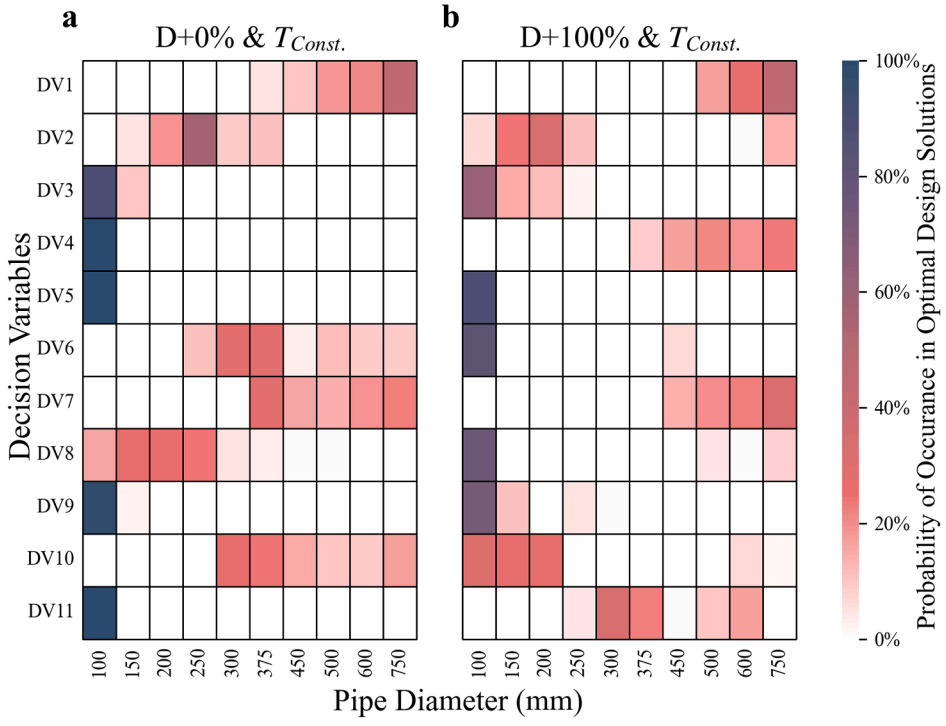

Fig. 10. Comparison of optimal solutions obtained under (a) D+0% & $T_{Const.}$ (b) D+100% & $T_{Const.}$ (Net1).

pipes connecting the other path between node 1 and 5 (i.e., DV7), there is a higher probability of pipe diameter larger than 500 mm being obtained for the later scenario mentioned above. These differences are mainly caused by the nature of a looped network, where water is likely to be delivered through different paths to a demand node (i.e., node 5 that has the highest demand in Net1 network) for meeting its demand. In this case, water is delivered either through DV2 & DV8 or through DV7 & DV4. While considering the overall pipe capital cost, the optimal solutions obtained under the three baseline demand scenarios all vary within a similar range of $\$0.4 \times 10^7$ to $\$1.2 \times 10^7$. This also indicates that the sizes of WDS optimised under different baseline demand scenarios are comparable. In addition, since the pump head required by the network is only determined by the hydraulics within the network, the pump selected will not be impacted by the solar PV integration either.

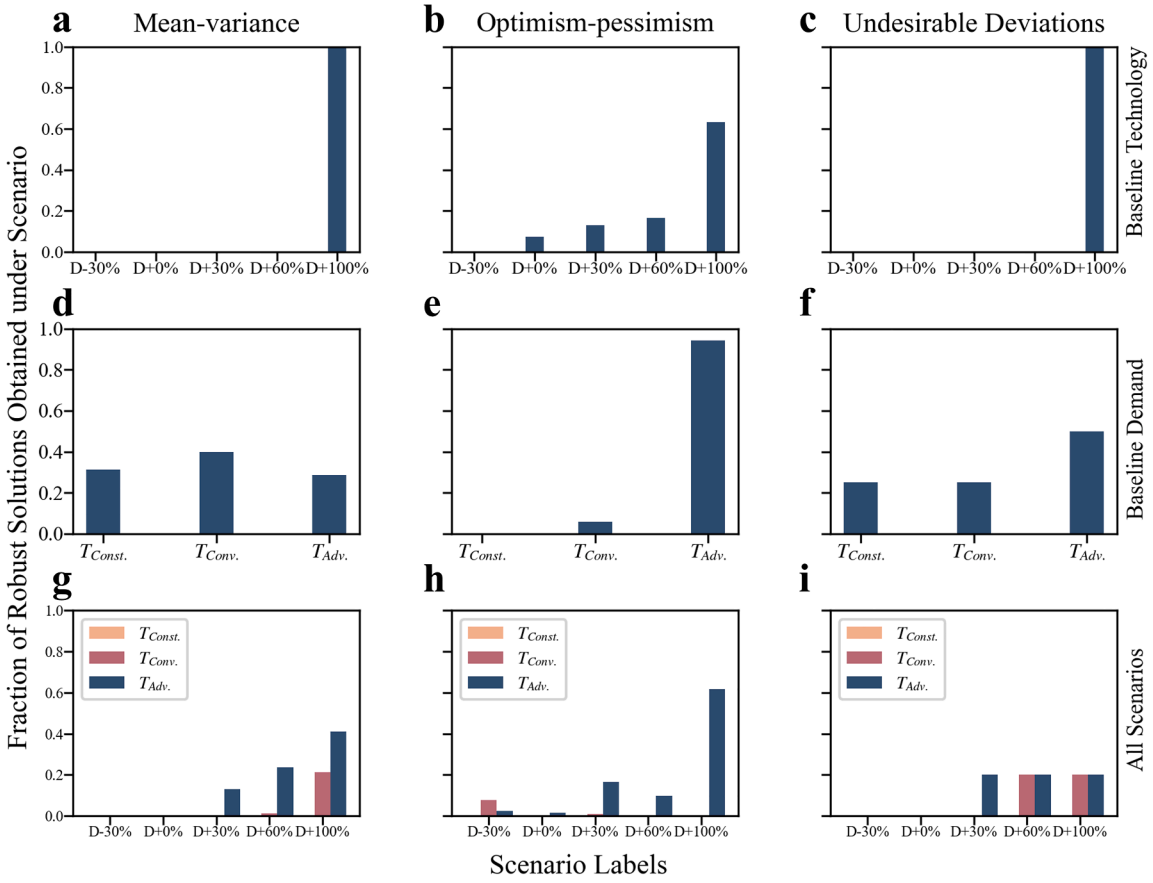

Fig. 11. Robust solutions identified using (a & d & g) Mean-variance, (b & e & h) Hurwicz Optimism-pessimism Rule, (c & f & i) Undesirable Deviations under (a-c) Five baseline technology scenarios, (d-f) three baseline demand scenarios, and (g-i) all 15 scenarios (Net1).

Therefore, the integration of BTM solar PV systems into WDSs, and the future development of solar PV technology has limited impact on the sizing of WDSs.

On the contrary, the pipe sizes of the WDS are significantly influenced by the future water demand considered when designing the system. The selection of pipe sizes for optimal solutions obtained under two baseline technology scenarios with the baseline and the largest demand growth (i.e., D+0% & $T_{const.}$ and D+100% & $T_{const.}$) for Net1 network are demonstrated in Fig. 10. The results illustrated in Fig. 10 clearly show that for pipes within the network, in general, relatively larger pipe sizes are chosen for optimal solutions obtained under baseline technology scenario with the higher demand growth. While some exceptions are observed, for example, pipe (i.e., DV8) connecting directly to the highest demand node (i.e., node 5) is more likely to be sized larger when there is no water demand change. This can be explained by changes in the delivery path for meeting the highest nodal demand and is mainly due to the nature of a looped network as discussed previously. More importantly, the trunk main pipe (i.e., DV1 in Net1 network, which connects the water source with the rest of the network) are generally sized with a much larger diameter of equal to or larger than 500 mm under the scenario with +100% demand growth, compared to the that of the scenario with +0% demand growth. This is because the trunk main pipe is sized to meet the total demand of the network, which is directly affected by the water demand growth considered. The optimal design solutions under the other three technology baseline scenarios for Net1 are illustrated in Fig. C.6. And similar results have been found for the Anytown network (see Fig. C.7 – Fig. C.9 in Appendix C).

4.2. Impact of robustness metrics on the selection of robust solutions

The robustness of optimal solutions obtained under (1) five baseline technology scenarios (i.e., D-30% & $T_{Const.}$, D+0% & $T_{Const.}$, D+30% & $T_{Const.}$, D+60% & $T_{Const.}$, D+100% & $T_{Const.}$), (2) three baseline demand scenarios (i.e., D+0% & $T_{Const.}$, D+0% & $T_{Conv.}$, D+0% & $T_{Adv.}$), and (3) the 15 scenarios have all been evaluated using the three different robustness metrics (referred to as Mean-variance, Hurwicz optimism-pessimism rule, and Undesirable deviations and discussed in Section 3.5). Robust solutions have been identified as well from the optimal solutions for the three groups of scenarios. The identified robust solutions are summarised based on the scenarios under which these solutions are obtained from, as shown in Figs. 11 and 12 for the two case studies.

As can be observed in the figures, it is obvious that the robust solutions identified using various robustness metrics come from optimal solutions obtained under different scenarios. When only considering the baseline technology scenarios within the design period, 100% of robust solutions come from the optimal solutions obtained under the highest demand growth scenario when the robustness is evaluated using mean-variance and undesirable deviations (Figs. 11(a) & (c), 12(a) & (c)). In addition, when Hurwicz optimism-pessimism rule is applied, as illustrated in Figs. 11(b) and 12(b), up to 60% of optimal solutions obtained under the largest demand growth scenarios are recognised as robust solutions. Thus, it is evident that optimal solutions resulting under larger water demand growth scenarios are generally identified as more robust solutions regardless of which robustness metric is considered. This is because designing for more extreme future water demand with larger capital costs spent for the network effectively reduces the risk of additional payments in terms of operational costs and operational energy consumed in the future. When considering technology development as

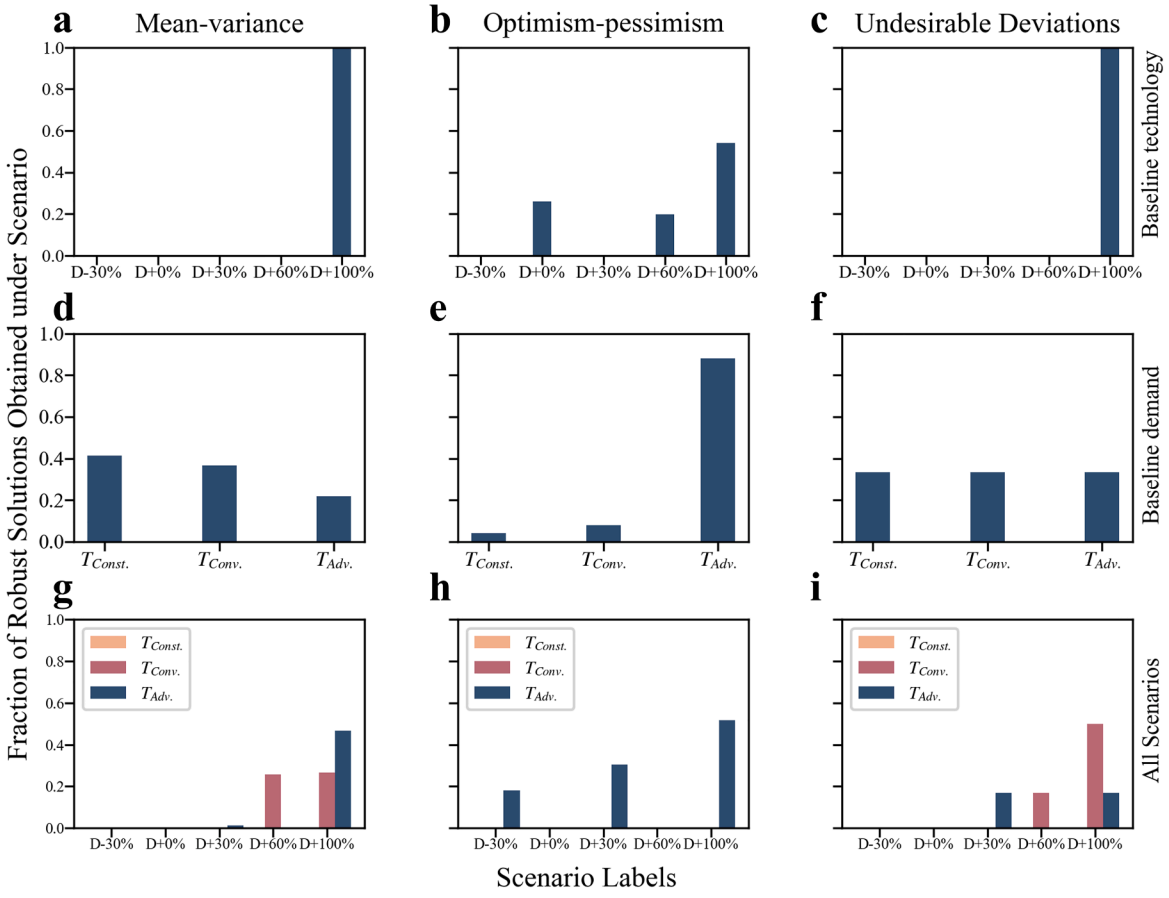

Fig. 12. Robust solutions identified using (a & d & g) Mean-variance, (b & e & h) Hurwicz Optimism-pessimism Rule, (c & f & i) Undesirable Deviations under (a-c) Five baseline technology scenarios, (d-f) three baseline demand scenarios, and (g-i) all 15 scenarios (Anytown).

the only source of uncertainty (i.e., the three baseline demand scenarios), only Hurwicz optimism-pessimism rule shows a clear preference for optimal solutions obtained under the advanced technology development scenario, as can be seen in Figs. 11(d)-(f) and 12(d)-(f). This could be explained by the change in the positions of robustness trade-offs. The development in solar PV technology significantly improves the robustness of energy performances (i.e., robustness of TGEC) of the network, with the cost of slight deterioration in the robustness of economic performances (i.e., robustness of TLCC). For a particular network design configuration, solar PV system generation capacity determined under more developed technology scenarios (e.g., $T_{Adv.}$ compared to $T_{conv.}$) would be smaller, due to its higher conversion efficiency and lower unit cost expected. Therefore, more developed solar technology scenarios tend to yield to solutions with smaller capital investment while ensuring relatively high solar PV generation utilisation.

The effects of technology development on the operational costs and energy consumption together impact the robustness evaluations of optimal solutions. In consideration of the uncertainty related to both demand and solar PV technology (i.e., robustness evaluation considering all 15 scenarios), as shown in Figs. 11(g)-(i) and 12(g)-(i), the development of solar technology enables more optimal solutions obtained under lower demand growth scenarios to be identified as robust solutions. This is explained by the large reduction in grid energy consumed by the WDS as well as the improved solar energy utilisation efficiency due to the development in solar technology. These improvements together make up for the potential additional operational energy required than expected caused by an underestimation of future demand when designing the WDS. As a result, lower capital cost solutions provided by optimisation under scenarios with lower demand growth become robust solutions when considering solar PV technology development. These solutions are usually characterised by considerably lower grid energy consumed under all plausible future scenarios. To some extent, the better energy performance of these solutions offsets their worse economic performance and thus recognises them as non-dominate robust solutions across all plausible future scenarios.

When assessing the performance of optimisation optimal solutions across the combined scenarios, the robustness metrics considered have been calculated, the calculated robustness results for both case studies are included as Fig. C.10 and Fig. C.11 in Appendix C. Three robustness metrics generally provide quite different trade-offs between the robustness of the two objective functions. To investigate the impact of robustness metrics selection on the resulted robustness trade-off, robustness calculations for optimal solutions obtained under highest demand growth and advanced technology development scenario (i.e., *D*+100% & $T_{Adv.}$) are demonstrated as an example in Fig. 13. Similar results for the Anytown network are obtained as shown in Fig. C.13.

As can be seen in Fig. 13, the robustness trade-offs between the calculated robustness of TLCC and TGEC using various robustness metrics (i.e., Mean-variance, Hurwicz optimism-pessimism rule, and Undesirable deviations) are completely different. Compared to the optimisation trade-off between the two objectives of TLCC and TGEC, the Pareto optimality of the original optimisation is preserved when assessing robustness using Hurwicz optimism-pessimism rule, as illustrated in Fig. 13(b) & (e). In more detail, the trade-off between the two robustness values is almost identical to the trade-off between the original optimisation trade-off between the objectives, with almost all the Pareto optimal optimisation solutions forming a clear Pareto front for the robustness trade-off. On the contrary, the Pareto-optimality of the original optimisation trade-off completely changed when Undesirable deviations is applied as the robustness metrics, as shown in Fig. 13(c) &

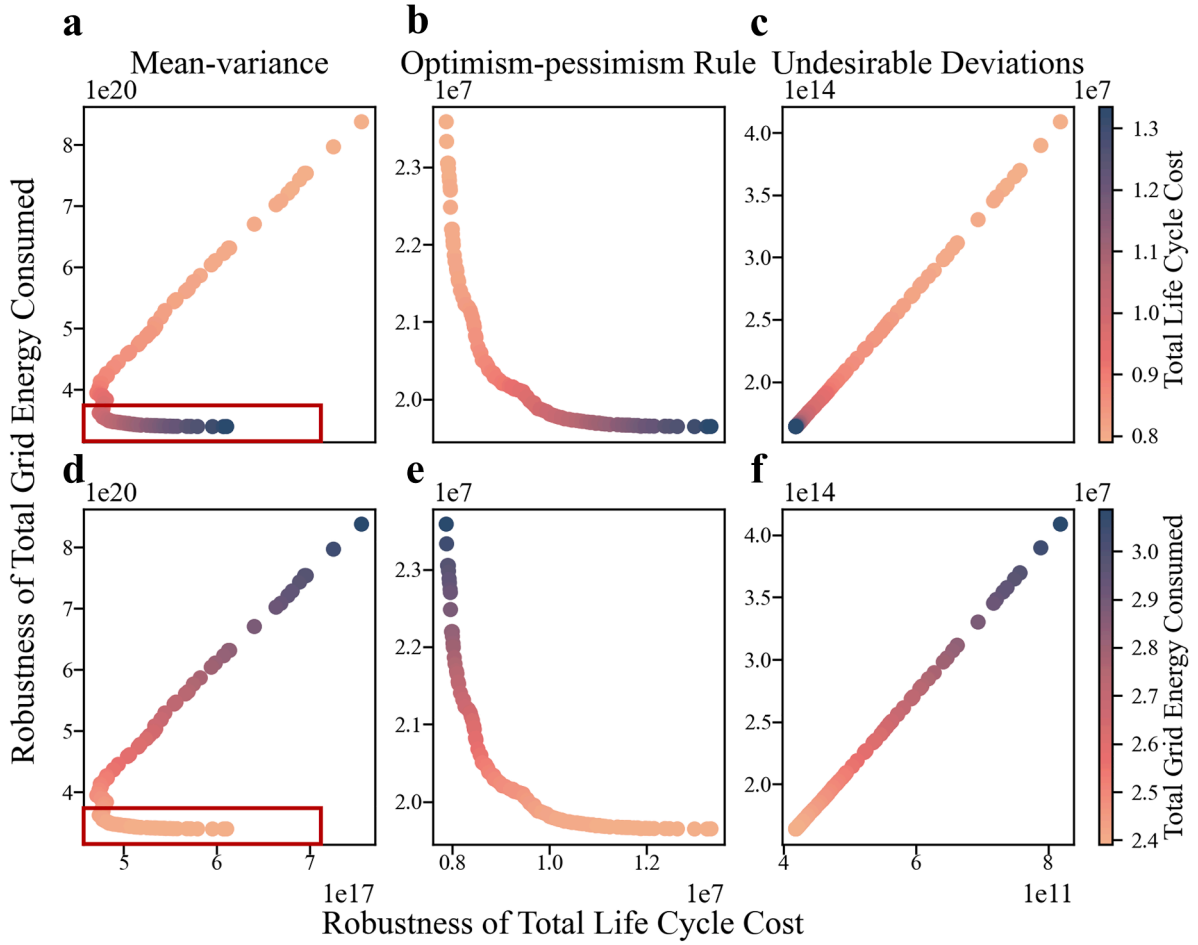

Fig. 13. Robustness evaluation using (a & d) Mean-variance, (b & e) Hurwicz Optimism-pessimism Rule, and (c & f) Undesirable deviations of optimal solutions obtained under D+100% & $T_{adv.}$ against (a-c) optimisation objective of total life cycle cost, (d-f) optimisation objective of total grid energy consumed (Net1).

(f). The result shows that the undesirable deviations of TLCC of the optimal solutions are positively related to the solutions' Undesirable deviations of TGEC, which means solutions with more robust in terms of TLCC are viewed as more robust considering TGEC as well. While mean-variance robustness metric shows mixed behaviour when evaluating the robustness of optimal design solutions, as can be seen in Fig. 13(a) & (d).

The robustness trade-offs are further related to the optimisation objectives, as illustrated in Fig. 13 with the colours of each solution related to its TLCC (Fig. 13(a)-(c)) and TGEC (Fig. 13(d)-(f)). Hurwicz optimism-pessimism rule robustness metric identified all the solutions obtained under the current scenario as non-dominated robust solutions. This indicates Hurwicz optimism-pessimism rule is not able to distinguish amongst optimal optimisation solutions. While undesirable deviations only recognise the largest cost with the lowest grid energy consumed solution as the robust solution, as highlighted in red square in Fig. 13(c) & (f). Since mean-variance robustness partially changes the optimisation optimality, as can be seen in Fig. 13(a) & (d), the larger cost with lower grid energy consumed part of optimal optimisation solutions (lower part of the trade-off, which is marked in red) are identified as equally robust in this case. Therefore, although the available optimal solutions for robustness evaluation are the same, the selection of different robustness metrics may lead to very different solutions identified as robust solutions.

Robustness metrics are calculated based on the statistical characteristics of the optimal solutions' performances under different scenarios. The differences in evaluation results are basically due to the different focuses of the various robustness metrics during calculation based on performances across all 15 scenarios. The distribution of TLCC (Fig. 11(a)) and TGEC (Fig. 11(b)) of all optimal solutions obtained under one scenario (i.e., D+100% & $T_{adv.}$) across the 15 scenarios for Net1 are illustrated in Fig. 14.

From the results demonstrated in Fig. 14, it is obvious that optimal solutions with larger average TLCC generally have smaller variations in TLCC across the 15 scenarios. While optimal solutions with larger average TGEC also have a wider range of performance across all scenarios. Since the improvement in mean performance (i.e., smaller average TGEC) agrees with the better performance in the range of TGEC (i.e., smaller variation in TGEC across 15 combined scenarios), this leads to the lower TGEC solutions are always preferred no matter which robustness metrics are considered. The lower TGEC solutions that are considered more robust in terms of their performances across all scenarios also in line with the preference of optimisation optimality, where solutions with smaller TGEC are preferred. However, considering TLCC, the robustness in terms of the TLCC of optimal solutions depends largely on the robustness metric calculations. Robustness metric such as Hurwicz optimism-pessimism rule, which is calculated reflecting the average performance of solutions' performances across all scenarios, the robust solution identified is generally consistent with the original optimality of the optimisation. This is because the average performance decreases with the decreasing optimisation objective of TLCC, as shown in Fig. 14(a). As both the Hurwicz optimism-pessimism rule robustness of TLCC and TGEC agree with the optimality of optimisation objectives of TLCC and TGEC, the Pareto optimality remains unchanged after the robustness evaluation. In comparison, undesirable deviations focuses on the range of the worst half of solutions' performances across all 15 scenarios, and as a result it provides totally opposite optimality

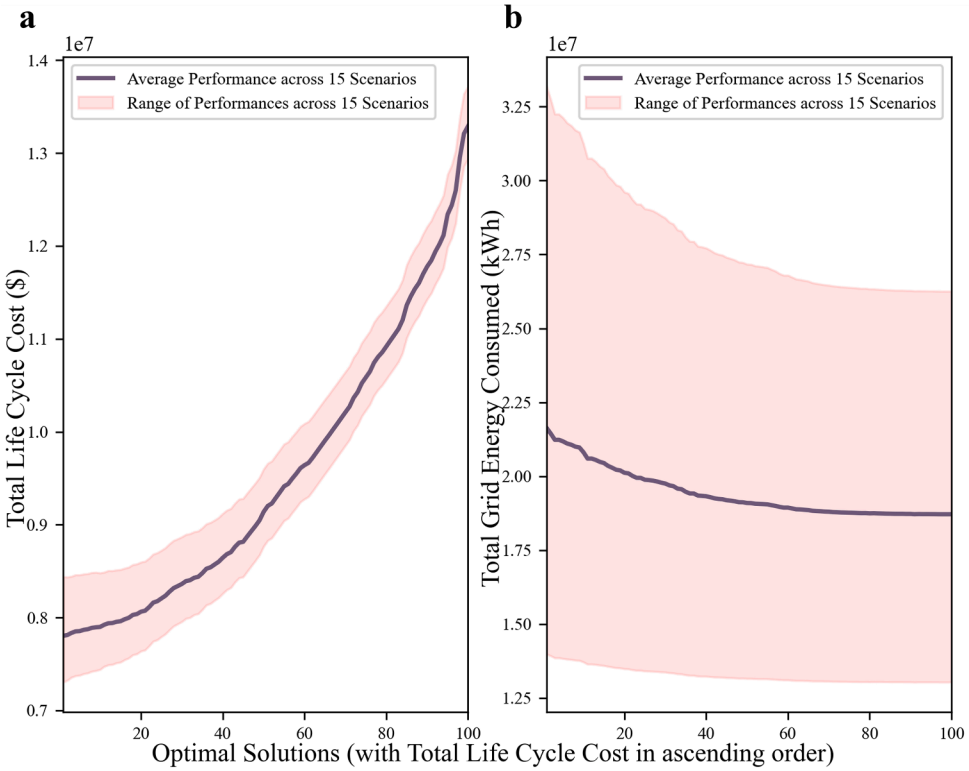

Fig. 14. Distribution of performances (a) optimisation objective of total life cycle cost, (b) optimisation objective of total grid energy consumed of optimal solutions obtained under D+100% & $T_{adv.}$ across all 15 scenarios (Net1).

compared to the objective of TLCC. Trade-offs between totally opposite preference in robustness of TLCC and entirely the same preference in robustness of TGEC, the Pareto optimality completely changes when applying Undesirable deviations for robustness evaluation. Mean-variance robustness assesses both the mean and the range of optimal solutions' performance across all scenarios, this leads to a changing point in the middle of the trade-off, as demonstrated in Fig. 14(a) & (d). The mean-variance robustness of TLCC of the upper part (i.e., optimal solutions with smaller TLCC and larger TGEC) is dominated by the larger variance, which pushes these solutions to dominated solution region. While the mean-variance robustness of TLCC of the lower part (i.e., optimal solutions with larger TLCC and smaller TGEC) is dominated by the larger average, and these solutions are pushed downwards by the superior robustness of TGEC. The robustness evaluation results indicate that the selection of robustness metrics will have a major impact on the robust solutions identified through changing of the Pareto optimality between the objectives. As different robustness metrics focus on different aspects of the statistical characteristics of optimal design solutions' performances distribution across the scenarios considered. Moreover, the formulation of the optimisation problem and the future scenarios developed for the robustness evaluation problem may also have an impact on the robustness assessment, as it impacts the performance distribution across scenarios.

In summary, the robustness evaluation of optimal solutions optimised under all 15 scenarios using different robustness metrics provide very different results, which leads to totally different design solutions for the WDS. However, despite various robustness metrics applied, the development in solar PV technology is always beneficial to improving the overall robustness of WDS under long-term demand change uncertainty. By considering solar PV technology development in the co-design of WDS integrating BTM solar, a wider variety of design solutions are offered as robust solutions. Especially more design solutions obtained under scenarios with lower water demand growth are identified as robust solutions considering all plausible long-term changes in water demand. This clearly shows the ability of BTM solar PV integration to improve the performance of WDSs across a range of uncertain future conditions through sustainable energy supply to the systems. Nevertheless, it also provides more sustainable and resilient design choices for decision-makers when designing future WDSs under changing water demand conditions. More importantly, integrating BTM solar PV system into existing WDSs that are already in place, where the water demand was underestimated when the WDS was designed, is beneficial as well. As these systems are supposed to serve people in the longer term into the future, it is critical that these systems can maintain their level of service while still being sustainable and energy efficient. A BTM solar PV system has been identified as a good option for improving WDS's resilience through considerable operational energy savings from the centralised electricity grid with little additional investment.

5. Conclusions

The energy supply and demand balance amongst varying pumping energy demand, intermittent solar energy generation, and the centralised electricity grid impacts the design of Behind-the-metre (BTM) solar integrated water distribution systems (WDSs). Long-term uncertainty in water demand and solar PV technology development further complicates the design optimisation problem. This paper proposes a co-design approach to incorporate the BTM solar PV system as an additional electricity supply to the design of WDSs under long-term water demand and solar PV technology development uncertainty. The WDS design problem has been formulated as a multi-objective optimisation problem, focusing on two objectives: minimising total life cycle cost and minimising total grid energy consumed. In addition, the BTM solar PV system sizing is included in the optimisation as a dependant variable. Fifteen scenarios representing the plausible future conditions for the BTM solar integrated WDSs have been developed, taking account of the long-term water demand change and solar PV technology development. Two benchmark case studies have been studied to demonstrate the co-design

approach and conduct analyses. Three different robustness metrics have been used to evaluate the design solutions performances across all scenarios, and further to investigate the impact of different robustness metrics on the identified robust design solutions.

In this study, both case study networks have been optimised under five baseline technology scenarios and three baseline demand scenarios. By comparing the optimal sizing of pipes within the networks under the two groups of scenarios, it has been found that the BTM solar PV integration has limited impact on the optimal WDS design. However, the optimal sizes of pipes and pumps for WDS are significantly affected by the changes in water demand conditions of the system into the future. The pipes are generally sized larger for scenarios with higher water demand growth expected in the longer-term, and this is more obvious for the trunk main pipe size selection within the WDS. Three robustness metrics emphasising different characteristics of the optimal solutions performances distribution across the 15 scenarios have been applied to obtain robust solutions from the optimisation optimal solutions. Based on the robust evaluation results, it is evident that different robustness metrics applied will lead to very different robust solutions identified. The Pareto optimality of the trade-off between the two robustness values calculated for the optimisation optimal solutions also varies when different robustness metrics are used. However, regardless of which robustness metric selected, the integration of BTM solar PV system and its associated technology development can effectively improve the robustness of WDS with uncertain water demand in the future.

The results of this study clearly point out the potential for improvements in WDS's energy performances under changing future conditions by integrating the BTM solar PV system as an additional source of energy supply. For WDSs that are already built and put in operation, BTM solar PV system is viewed as a good add-on component. As the BTM solar PV system is flexible to be customised based on the energy demand of the WDS with little economic investment, while it greatly improves the WDS's energy performance in return. Moreover, the potential decrease in cost and increase in conversion efficiency of solar PV modules are proven to effectively increase WDS design solutions' robustness across varying water demand change conditions in future through the improved energy performances of the system. The continuously lowering reliant on centralised grid energy of the WDS and increasing BTM solar PV generation penetration to the WDS also help reduce the risk of oversizing the WDS's components (i.e., pipes) when designing a new WDS. This is because lower capital cost design solutions performs consistently better across potential future water demand change conditions, which makes them become more feasible solutions for decision-makers. This highlights the potential opportunity of maintaining or even improving system performance under changed future demand by integrating BTM solar PV to originally under-sized WDSs, improving the WDS's robustness from an energy perspective.

However, there are still limitations in this study which could be considered in future research. First, only a certain proportion of BTM solar PV generation could be utilised by the WDS, due to the temporal mismatch between the BTM solar PV generated energy supply and the WDS pumping energy demand. Adding an energy storage system such as a battery is considered a better way to make use of the BTM solar PV system. In addition, making use of elevated water storages in a WDS is another potential option to maximise the benefits from the BTM solar energy generated and improve overall system efficiency. The design of the energy storage system together with the BTM solar PV system, and the interactions amongst energy demand, energy supply, and energy storage could be considered in future works. Furthermore, as discussed in this study, the selection of robustness metrics for assessing design solutions' performances across a range of future conditions significantly impacts the solutions' optimality and the final identified solutions. Therefore, a comprehensive study focusing on the impact of different robustness metrics on the identified robust solutions, and the characteristics of the robust solutions could be useful for guiding decision-making in the future.

This study investigates the optimal design of future WDSs, which are important infrastructure affecting the everyday life of people in cities. By integrating BTM solar PV systems, the environmental impact of WDSs due to the consumption of energy generated from fossil fuels is effectively reduced. By considering potential changes in future system operation conditions induced by various human activities, robust WDSs can be designed so that their level of service to consumers can be maintained into the future. More importantly, the implications of the major findings from this study are not only restricted to WDSs, they can also be extended to provide insightful information for decision-makers when designing other critical infrastructure for future cities.

Declaration of Competing Interest

The authors declare the following financial interests/personal relationships which may be considered as potential competing interests: Wenyan Wu reports financial support was provided by Australian Research Council.

Data availability

Data will be made available on request.

Acknowledgement

Jiayu Yao acknowledges support from The University of Melbourne via the Melbourne Research Scholarship. Wenyan Wu acknowledges support from the Australian Research Council via the Discovery Early Career Researcher Award (DE210100117). This research is supported by The University of Melbourne's Research Computing Services and the Petascale Campus Initiative.

Appendix A. Solar PV system generation patterns

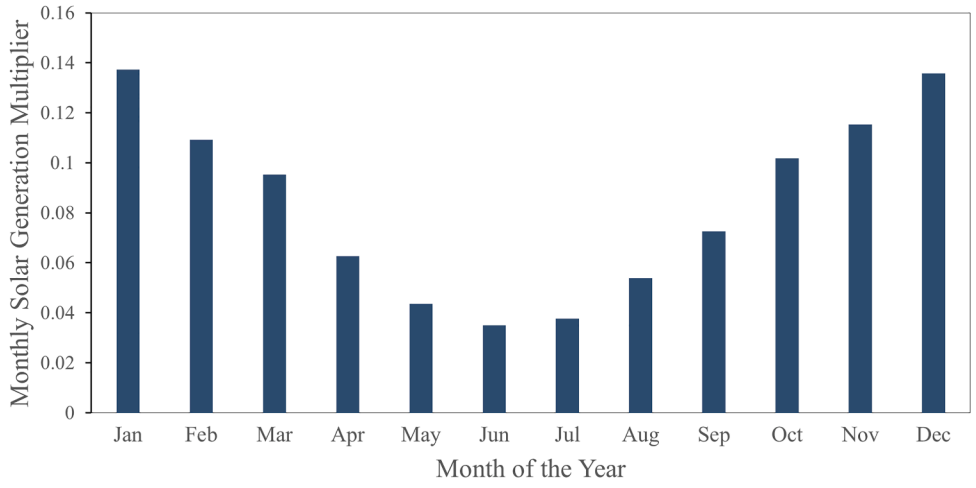

Fig. A.1. Solar PV system monthly generation pattern (Melbourne, Australia).

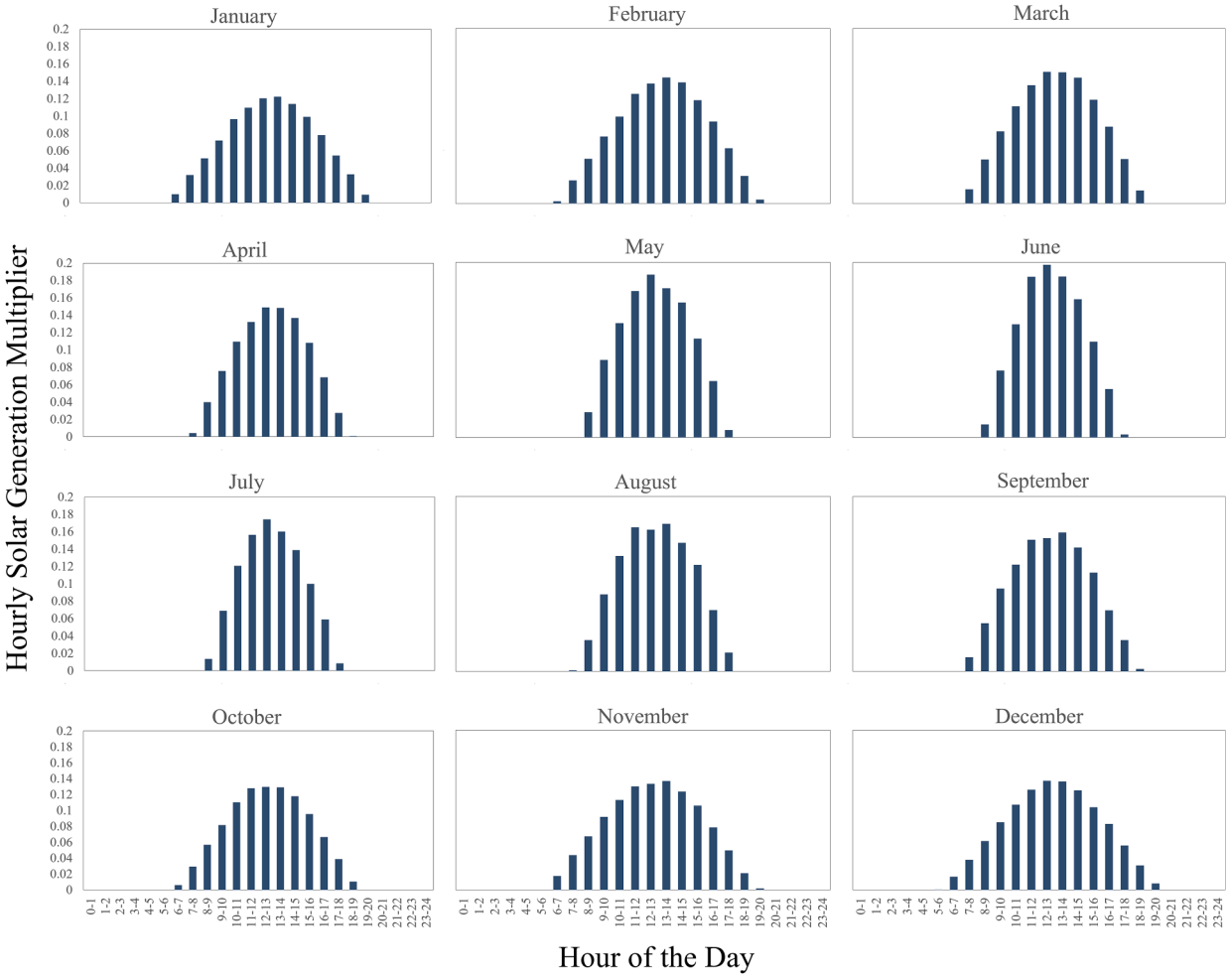

Fig. A.2. Solar PV system diurnal generation patterns for different months.

Appendix B. Simulation of variable speed pump and pump power estimation

In this research, water is pumped from a single source to the demand nodes without storage tanks or reservoirs that may affect the hydraulics of pipe flow in the network. Therefore, the nodal heads in the network are linearly correlated to the pump head provided by the pump station. A simplification method for simulation of Variable Speed Pump (VSP) is proposed here. A Pressure Reducing Valve (PRV) is applied instead of a fixed speed pump with pre-determined pump curves to simulate the adjustments of pump speed in the hydraulic solver.

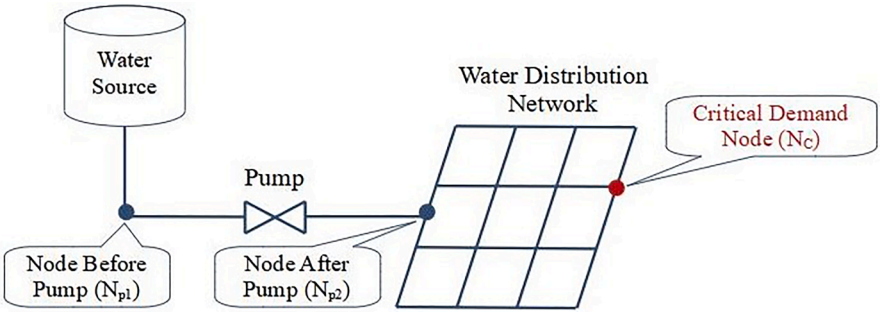

Fig. B.1. Simulation of variable speed pump.

As illustrated in Fig. B.1, the water distribution network is connected to a water source by a pump represented as a PRV. The pressure head provided by the water source is set to be high enough for the system, which is the head before the PRV. Meanwhile, the pressure head after the PRV is expressed as the PRV setting in EPANET, and the pump head provided could be calculated as the pressure difference before and after the PRV. The PRV setting is adjusted to ensure the pressure head of the critical demand node (node with minimum pressure head in the network) always remains to be equal and higher than the minimum allowable head of 28 m of water(Ghorbanian et al., 2015). The pump head at each simulation time-step could be calculated using the following equations:

$$\Delta H = H_{N_C} - H_{min} \tag{B.1}$$

$$H_{pump} = \left(H_{N_{p1}} - H_{N_{p2}}\right) - \Delta H \tag{B.2}$$

Where, ΔH is the pressure deficit of the network, which is expressed as the difference between the minimum allowable pressure head (H_{min}) and the actual pressure head of the critical demand node; H_{pump} is the adjusted pump head.

The pump power for each simulation time-step could then be calculated using the pump head determined and the flow delivered by the pump according to the network requirements. The size of the VSP will be characterised by the maximum pump power within the pump's service lifespan.

Supplementary materials

Supplementary material associated with this article can be found, in the online version, at doi:10.1016/j.scs.2023.104844.

References

Abelson, P., & Dalton, T. (2018). Choosing the social discount rate for Australia. *Australian Economic Review, 51*(1), 52–67. https://doi.org/10.1111/1467-8462.12254

Angizeh, F., Ghofrani, A., Zaidan, E., & Jafari, M. A. (2021). Resilience-oriented behind-the-meter energy storage system evaluation for mission-critical facilities. *IEEE access : practical innovations, open solutions, 9*, 80854–80865. https://doi.org/10.1109/ACCESS.2021.3085410

Arora, M., Malano, H., Davidson, B., Nelson, R., & George, B. (2015). Interactions between centralized and decentralized water systems in urban context: A review. *Wiley Interdisciplinary Reviews: Water, 2*(6), 623–634. https://doi.org/10.1002/wat2.1099

Ávila, C. A. M., Sánchez-Romero, F.-J., López-Jiménez, P. A., & Pérez-Sánchez, M. (2022). Improve leakage management to reach sustainable water supply networks through by green energy systems. Optimized case study. *Sustainable Cities and Society, 83*, Article 103994. https://doi.org/10.1016/j.scs.2022.103994

Basupi, I., & Kapelan, Z. (2015). Flexible water distribution system design under future demand uncertainty. *Journal of water resources planning and management, 141*(4), Article 04014067. https://doi.org/10.1061/(ASCE)WR.1943-5452.0000416

Bayram, I. S., & Ustun, T. S. (2017). A survey on behind the meter energy management systems in smart grid. *Renewable and Sustainable Energy Reviews, 72*, 1208–1232. https://doi.org/10.1016/j.rser.2016.10.034

Beal, C. D., & Stewart, R. A. (2014). Identifying residential water end uses underpinning peak day and peak hour demand. *Journal of Water Resources Planning and Management, 140*(7), Article 04014008. https://doi.org/10.1061/(ASCE)WR.1943-5452.0000357

Behandish, M., & Wu, Z. Y. (2014). Concurrent pump scheduling and storage level optimization using meta-models and evolutionary algorithms. *Procedia Engineering, 70*, 103–112. https://doi.org/10.1016/j.proeng.2014.02.013

Blank, J., & Deb, K. (2020). Pymoo: Multi-objective optimization in python. *IEEE access : practical innovations, open solutions, 8*, 89497–89509. https://doi.org/10.1109/ACCESS.2020.2990567

Bolinger, M., Seel, J., & Wu, M. (2016). Maximizing MWh: A statistical analysis of the performance of utility-scale photovoltaic projects in the United States. In *2016 IEEE 43rd Photovoltaic Specialists Conference (PVSC)*.

Boretti, A., & Rosa, L. (2019). Reassessing the projections of the world water development report. *NPJ Clean Water, 2*(1), 1–6. https://doi.org/10.1038/s41545-019-0039-9

Carrillo-Cobo, M. T., Camacho-Poyato, E., Montesinos, P., & Díaz, J. A. R. (2014). Assessing the potential of solar energy in pressurized irrigation networks. The case of Bembézar MI irrigation district (Spain). *Spanish Journal of Agricultural Research, 12*(3), 838–849. https://doi.org/10.5424/sjar/2014123-5327

Clean Energy Council. (2020). *Guide to installing solar pv for business and industry*. Clean Energy Council. Issue.

Coelho, B., & Andrade-Campos, A. (2014). Efficiency achievement in water supply systems—A review. *Renewable and Sustainable Energy Reviews, 30*, 59–84. https://doi.org/10.1016/j.rser.2013.09.010

Creaco, E., Franchini, M., & Walski, T. (2015). Taking account of uncertainty in demand growth when phasing the construction of a water distribution network. *Journal of water resources planning and management, 141*(2), Article 04014049. https://doi.org/10.1061/(ASCE)WR.1943-5452.0000441

Cunha, M., Marques, J., Creaco, E., & Savić, D. (2019). A dynamic adaptive approach for water distribution network design. *Journal of water resources planning and management, 145*(7), Article 04019026. https://doi.org/10.1061/(ASCE)WR.1943-5452.0001085

Cunha, M., Marques, J., & Savić, D. (2020). A flexible approach for the reinforcement of water networks using multi-criteria decision analysis. *Water Resources Management, 34*(14), 4469–4490. https://doi.org/10.1007/s11269-020-02655-9

Deb, K., Pratap, A., Agarwal, S., & Meyarivan, T. (2002). A fast and elitist multiobjective genetic algorithm: NSGA-II. *IEEE Transactions on Evolutionary Computation, 6*(2), 182–197. https://doi.org/10.1109/4235.996017

De Marchis, M., Fontanazza, C., Freni, G., Messineo, A., Milici, B., Napoli, E., Notaro, V., Puleo, V., & Scopa, A. (2014). Energy recovery in water distribution networks. Implementation of pumps as turbine in a dynamic numerical model. *Procedia Engineering, 70*, 439–448. https://doi.org/10.1016/j.proeng.2014.02.049

Department of Primary Industries. (2014). *NSW reference rates manual - Valuation of water supply, sewerage and stormwater assets*.

Doyle, M. W., & Havlick, D. G. (2009). Infrastructure and the environment. *Annual Review of Environment and Resources, 34*, 349–373.

Energy Sector Management Assistance Program. (2020). *Global photovoltaic power potential by country*. World Bank. https://doi.org/10.1596/34102

EPA. (2022). *Drinking water distribution systems*. July 8, 2022. United States Environmental Protection Agency https://www.epa.gov/dwsixyearreview/drinking-water-distribution-systems.

Essential Services Commission. (2021). *Victorian default offer*. https://www.esc.vic.gov.au/electricity-and-gas/prices-tariffs-and-benchmarks/victorian-default-offer.

Garcia, A. V. M., López-Jiménez, P. A., Sánchez-Romero, F.-J., & Pérez-Sánchez, M (2021). Objectives, keys and results in the water networks to reach the sustainable development goals. *Water, 13*(9), 1268. https://doi.org/10.3390/w13091268

Gato, S., Jayasuriya, N., & Roberts, P. (2007). Forecasting residential water demand: Case study. *Journal of Water Resources Planning and Management, 133*(4), 309–319. https://doi.org/10.1061/(ASCE)0733-9496(2007)133:4(309)

Gato-Trinidad, S., & Gan, K. (2012). Characterizing maximum residential water demand. *Urban Water, 122*, 15–24. https://doi.org/10.2495/UW120021

Ghorbanian, V., Karney, B., & Guo, Y. (2015). Minimum pressure criterion in water distribution systems: Challenges and consequences. *World environmental and water resources congress 2015*.

Giudici, F., Castelletti, A., Garofalo, E., Giuliani, M., & Maier, H. R. (2019). Dynamic, multi-objective optimal design and operation of water-energy systems for small, off-grid islands. *Applied Energy, 250*, 605–616. https://doi.org/10.1016/j.apenergy.2019.05.084

Gowrisankaran, G., Reynolds, S. S., & Samano, M. (2016). Intermittency and the value of renewable energy. *Journal of Political Economy, 124*(4), 1187–1234. https://doi.org/10.1086/686733

Green, M. A. (2001). Third generation photovoltaics: Ultra-high conversion efficiency at low cost. *Progress in Photovoltaics: Research and Applications, 9*(2), 123–135. https://doi.org/10.1002/pip.360

Gul, M., Kotak, Y., & Muneer, T. (2016). Review on recent trend of solar photovoltaic technology. *Energy Exploration & Exploitation, 34*(4), 485–526. https://doi.org/10.1177/0144598716650552

Hamiche, A. M., Stambouli, A. B., & Flazi, S. (2016). A review of the water-energy nexus. *Renewable and Sustainable Energy Reviews, 65*, 319–331. https://doi.org/10.1016/j.rser.2016.07.020

Hurwicz, L. (1951). *Optimality criteria for decision making under ignorance*.

International Renewable Energy Agency. (2019). Future of solar photovoltaic: Deployment, investment, technology, grid integration and socio-economic aspects. *A global energy transformation*.

Kraft, D. (1988). A software package for sequential quadratic programming. *Forschungsbericht- Deutsche Forschungs- und Versuchsanstalt fur Luft- und Raumfahrt*.

Kwakkel, J. H., Eker, S., & Pruyt, E. (2016). How robust is a robust policy? Comparing alternative robustness metrics for robust decision-making. *Robustness Analysis in Decision Aiding, Optimization, and Analytics*, 221–237. https://doi.org/10.1007/978-3-319-33121-8_10

Kwakkel, J. H., Walker, W. E., & Marchau, V. A. (2010). Classifying and communicating uncertainties in model-based policy analysis. *International Journal of Technology, Policy and Management, 10*(4), 299–315. https://doi.org/10.1504/IJTPM.2010.036918

Lempert, R.J. (2003). Shaping the next one hundred years: New methods for quantitative, long-term policy analysis.

Letting, L. K., Hamam, Y., & Abu-Mahfouz, A. M. (2017). Estimation of water demand in water distribution systems using particle swarm optimization. *Water, 9*(8), 593. https://doi.org/10.3390/w9080593

Luna, T., Ribau, J., Figueiredo, D., & Alves, R. (2019). Improving energy efficiency in water supply systems with pump scheduling optimization. *Journal of Cleaner Production, 213*, 342–356. https://doi.org/10.1016/j.jclepro.2018.12.190

Maier, H. R., Guillaume, J. H., van Delden, H., Riddell, G. A., Haasnoot, M., & Kwakkel, J. H. (2016). An uncertain future, deep uncertainty, scenarios, robustness and adaptation: How do they fit together? *Environmental Modelling & Software, 81*, 154–164. https://doi.org/10.1016/j.envsoft.2016.03.014

Maier, H. R., Razavi, S., Kapelan, Z., Matott, L. S., Kasprzyk, J., & Tolson, B. A. (2019). Introductory overview: Optimization using evolutionary algorithms and other metaheuristics. *Environmental Modelling & Software, 114*, 195–213. https://doi.org/10.1016/j.envsoft.2018.11.018

Marchi, A., Simpson, A. R., & Ertugrul, N. (2012). Assessing variable speed pump efficiency in water distribution systems. *Drinking Water Engineering and Science, 5*(1), 15–21. https://doi.org/10.5194/dwes-5-15-2012

Marques, J., Cunha, M., & Savić, D. (2015a). Using real options in the optimal design of water distribution networks. *Journal of Water Resources Planning and Management, 141*(2), Article 04014052. https://doi.org/10.1061/(ASCE)WR.1943-5452.0000448

Marques, J., Cunha, M., & Savić, D. (2018). Many-objective optimization model for the flexible design of water distribution networks. *Journal of Environmental Management, 226*, 308–319. https://doi.org/10.1016/j.jenvman.2018.08.054

Marques, J., Cunha, M., Savić, D., & Giustolisi, O. (2017). Water network design using a multiobjective real options framework. *Journal of Optimization, 2017*. https://doi.org/10.1155/2017/4373952

Marques, J., Cunha, M., & Savić, D. A. (2015b). Multi-objective optimization of water distribution systems based on a real options approach. *Environmental Modelling & Software, 63*, 1–13. https://doi.org/10.1016/j.envsoft.2014.09.014

McPhail, C., Maier, H., Kwakkel, J., Giuliani, M., Castelletti, A., & Westra, S. (2018). Robustness metrics: How are they calculated, when should they be used and why do they give different results? *Earth's Future, 6*(2), 169–191. https://doi.org/10.1002/2017EF000649

National Renewable Energy Laboratory. (2022). *Best research-cell efficiency chart*. https://www.nrel.gov/pv/cell-efficiency.html.

National Research Council. (2005). *Public water supply distribution systems: Assessing and reducing risks: First report*. National Academies Press.

National Research Council. (2007). *Drinking water distribution systems: Assessing and reducing risks*. National Academies Press.

National Solar Radiation Database. (2022). *Data-viewer*. https://nsrdb.nrel.gov/.

Okello, C., Tomasello, B., Greggio, N., Wambiji, N., & Antonellini, M. (2015). Impact of population growth and climate change on the freshwater resources of Lamu Island, Kenya. *Water, 7*(3), 1264–1290. https://doi.org/10.3390/w7031264

Olcan, C. (2015). Multi-objective analytical model for optimal sizing of stand-alone photovoltaic water pumping systems. *Energy Conversion and Management, 100*, 358–369. https://doi.org/10.1016/j.enconman.2015.05.018

Open Water Analytics. (2022a). *EPANET*. https://github.com/OpenWaterAnalytics/EPANET.

Open Water Analytics. (2022b). *epanet-python*. https://github.com/OpenWaterAnalytics/epanet-python.

PVC Pipe Association. (2017). *Ductile iron pipe's hazen-williams flow coefficient declines over time*.

Ramos, H. M., Kenov, K. N., & Vieira, F. (2011). Environmentally friendly hybrid solutions to improve the energy and hydraulic efficiency in water supply systems. *Energy for Sustainable Development, 15*(4), 436–442. https://doi.org/10.1016/j.esd.2011.07.009

Rathnayaka, K., Maheepala, S., Nawarathna, B., George, B., Malano, H., Arora, M., & Roberts, P. (2014). Factors affecting the variability of household water use in Melbourne, Australia. *Resources, Conservation and Recycling, 92*, 85–94. https://doi.org/10.1016/j.resconrec.2014.08.012

Rehman, S., & Sahin, A. Z. (2012). Wind power utilization for water pumping using small wind turbines in Saudi Arabia: A techno-economical review. *Renewable and Sustainable Energy Reviews, 16*(7), 4470–4478. https://doi.org/10.1016/j.rser.2012.04.036

Roberts, P. (2005). *Yarra valley water: 2004 residential end use measurement study*. Yarra Valley Water Melbourne.

Rossman, L.A. (2000). EPANET 2: Users manual.

Sharif, M. N., Haider, H., Farahat, A., Hewage, K., & Sadiq, R. (2019). Water–energy nexus for water distribution systems: A literature review. *Environmental Reviews, 27*(4), 519–544. https://doi.org/10.1139/er-2018-0106

Shubbak, M. H. (2019). Advances in solar photovoltaics: Technology review and patent trends. *Renewable and Sustainable Energy Reviews, 115*, Article 109383. https://doi.org/10.1016/j.rser.2019.109383

Simpson, A. R., Dandy, G. C., & Murphy, L. J. (1994). Genetic algorithms compared to other techniques for pipe optimization. *Journal of Water Resources Planning and Management, 120*(4), 423–443. https://doi.org/10.1061/(ASCE)0733-9496(1994)120:4(423

Sitzenfrei, R., & Rauch, W. (2015). Optimizing small hydropower systems in water distribution systems based on long-time-series simulation and future scenarios. *Journal of Water Resources Planning and Management, 141*(10), Article 04015021. https://doi.org/10.1061/(ASCE)WR.1943-5452.0000537

State of Victoria. (2016). *Water for victoria water plan*.

Terrill, M., & Batrouney, H. (2018). *Unfreezing discount rates: Transport infrastructure for tomorrow*. Australia: Grattan Institute Melbourne.

Tricarico, C., Morley, M. S., Gargano, R., Kapelan, Z., Savić, D., Santopietro, S., Granata, F., & De Marinis, G. (2018). Optimal energy recovery by means of pumps as turbines (PATs) for improved WDS management. *Water Science and Technology: Water Supply, 18*(4), 1365–1374. https://doi.org/10.2166/ws.2017.202

Tsegaye, S., Gallagher, K. C., & Missimer, T. M. (2020). Coping with future change: Optimal design of flexible water distribution systems. *Sustainable Cities and Society, 61*, Article 102306. https://doi.org/10.1016/j.scs.2020.102306

Victoria, M., Haegel, N., Peters, I. M., Sinton, R., Jäger-Waldau, A., del Cañizo, C., Breyer, C., Stocks, M., Blakers, A., & Kaizuka, I. (2021). Solar photovoltaics is ready to power a sustainable future. *Joule, 5*(5), 1041–1056. https://doi.org/10.1016/j.joule.2021.03.005

Virtanen, P., Gommers, R., Oliphant, T. E., Haberland, M., Reddy, T., Cournapeau, D., Burovski, E., Peterson, P., Weckesser, W., & Bright, J. (2020). SciPy 1.0: Fundamental algorithms for scientific computing in Python. *Nature Methods, 17*(3), 261–272. https://doi.org/10.1038/s41592-019-0686-2

Walski, T. M., Brill, E. D., Jr, Gessler, J., Goulter, I. C., Jeppson, R. M., Lansey, K., Lee, H.-L., Liebman, J. C., Mays, L., & Morgan, D. R. (1987). Battle of the network models: Epilogue. *Journal of Water Resources Planning and Management, 113*(2), 191–203. https://doi.org/10.1061/(ASCE)0733-9496(1987)113:2(191)

Walters, G. A., Halhal, D., Savic, D., & Ouazar, D. (1999). Improved design of "Anytown" distribution network using structured messy genetic algorithms. *Urban Water, 1*(1), 23–38. https://doi.org/10.1016/S1462-0758(99)00005-9

Wang, H., Yang, X., Lou, Q., & Xu, X. (2021). Achieving a sustainable development process by deployment of solar PV power in ASEAN: A SWOT analysis. *Processes, 9*(4), 630. https://doi.org/10.3390/pr9040630

Water Services Association of Australia. (2011). *Water supply code of Australia: Wsa 03-2011-3.1*.

Wu, W., Maier, H. R., Dandy, G. C., Arora, M., & Castelletti, A. (2020). The changing nature of the water–energy nexus in urban water supply systems: A critical review of changes and responses. *Journal of Water and Climate Change, 11*(4), 1095–1122. https://doi.org/10.2166/wcc.2020.276

Wu, W., Simpson, A. R., & Maier, H. R. (2010). Accounting for greenhouse gas emissions in multiobjective genetic algorithm optimization of water distribution systems. *Journal of Water Resources Planning and Management, 136*(2), 146–155. https://doi.org/10.1061/(ASCE)WR.1943-5452.0000020

WWAP. (2019). The United Nations world water development report. In *The United Nations world water development report, 507*.

Zhang, W., Chung, G., Pierre-Louis, P., Bayraksan, G., & Lansey, K. (2013). Reclaimed water distribution network design under temporal and spatial growth and demand uncertainties. *Environmental Modelling & Software, 49*, 103–117. https://doi.org/10.1016/j.envsoft.2013.07.008

Zhao, Q., Wu, W., Simpson, A. R., & Willis, A. (2023). Water distribution system optimization considering behind-the-meter solar energy with a hydraulic-power-based search space reduction method. *Journal of Water Resources Planning and Management*. https://doi.org/10.1061/JWRMD5/WRENG-5875

Zib, L., III, Byrne, D. M., Marston, L. T., & Chini, C. M (2021). Operational carbon footprint of the US water and wastewater sector's energy consumption. *Journal of Cleaner Production, 321*, Article 128815. https://doi.org/10.1016/j.jclepro.2021.128815